SIGNAL TRANSDUCTION

The β-catenin C terminus links Wnt and sphingosine-1-phosphate signaling pathways to promote vascular remodeling and atherosclerosis

Gustavo H. Oliveira-Paula[1], Sophia Liu[1], Alishba Maira[1], Gaia Ressa[1], Graziele C. Ferreira[1,2], Amado Quintar[1], Smitha Jayakumar[1], Vanessa Almonte[1], Dippal Parikh[1], Tomas Valenta[3], Konrad Basler[3], Timothy Hla[4], Dario F. Riascos-Bernal[1]*, Nicholas E. S. Sibinga[1]*

Copyright © 2024 The Authors, some rights reserved; exclusive licensee American Association for the Advancement of Science. No claim to original U.S. Government Works. Distributed under a Creative Commons Attribution NonCommercial License 4.0 (CC BY-NC).

Canonical Wnt and sphingosine-1-phosphate (S1P) signaling pathways are highly conserved systems that contribute to normal vertebrate development, with key consequences for immune, nervous, and cardiovascular system function; despite these functional overlaps, little is known about Wnt/β-catenin–S1P cross-talk. In the vascular system, both Wnt/β-catenin and S1P signals affect vessel maturation, stability, and barrier function, but information regarding their potential coordination is scant. We report an instance of functional interaction between the two pathways, including evidence that S1P receptor 1 (S1PR1) is a transcriptional target of β-catenin. By studying vascular smooth muscle cells and arterial injury response, we find a specific requirement for the β-catenin carboxyl terminus, which acts to induce S1PR1, and show that this interaction is essential for vascular remodeling. We also report that pharmacological inhibition of the β-catenin carboxyl terminus reduces S1PR1 expression, neointima formation, and atherosclerosis. These findings provide mechanistic understanding of how Wnt/β-catenin and S1P systems collaborate during vascular remodeling and inform strategies for therapeutic manipulation.

INTRODUCTION

Cardiovascular disease, the number one cause of death globally, is responsible for considerable morbidity and health care costs worldwide (*1*). Vascular remodeling is a hallmark of cardiovascular diseases including atherosclerosis, stenosis after angioplasty and stent placement, vein graft disease, and transplant arteriosclerosis (*2*). Smooth muscle cells (SMCs) contribute substantially to vascular remodeling induced by injury or disease (*2*, *3*). In normal arteries, SMCs are typically confined to the medial layer and regulate vessel tone or diameter (*2*, *3*). After vascular injury or during atherosclerosis, SMCs undergo phenotypic switching from a quiescent, differentiated, contractile, and nonmigratory phenotype to a dedifferentiated, migratory, proliferative, and secretory phenotype (*3*). These changes promote SMC proliferation and migration from the media into the intima, and lead to neointima formation that may occlude the arterial lumen (*3*). The molecular mechanisms underlying these processes are, however, not fully understood, which limits implementation of therapies to reduce vascular remodeling and disease.

Sphingosine-1-phosphate (S1P) is a bioactive sphingolipid that regulates a plethora of physiological and pathogenic processes in multiple organs (*4*). Generated by the phosphorylation of sphingosine by sphingosine kinases, S1P binds to five distinct G protein–coupled S1P receptors (S1PR1 to S1PR5) (*5*). S1P promotes vascular SMC proliferation and migration (*6*–*9*) and increases aortic intima-media thickness in animal models (*6*). Clinically, S1P serum levels are elevated in patients with coronary artery disease (*10*, *11*). In addition, circulating S1P concentrations are positively associated with a greater carotid intima-media thickness in the general population (*12*). S1P receptors—S1PR1, S1PR2, and S1PR3—have been implicated in vascular SMC proliferation and neointima formation (*13*–*17*). Wamhoff *et al.* (*14*) observed that vascular injury induced expression of S1PR1 and S1PR3 but reduced that of S1PR2. Further studies reported higher S1PR1 expression in injured arteries from both animals and humans (*16*–*18*). In addition, overexpression of S1PR1 increased SMC proliferation in culture (*13*) and enhanced arterial occlusion in vivo (*15*), while pharmacological inhibition of S1PR1 promoted opposite effects (*14*). Collectively, these findings suggest that S1P contributes to vascular remodeling by activating S1PR1. Accordingly, better understanding of how S1PR1 expression is regulated could have therapeutic implications for cardiovascular disease and other pathologies in which this signaling pathway is active.

In a previous study, we found that inactivation of β-catenin expression in vascular SMCs in culture decreased mRNA levels of *S1pr1* (*19*); the mechanistic basis and functional relevance of this finding has not been investigated. β-Catenin plays a dual role in the cell (*20*, *21*), serving as a structural component of cadherin-based adherens junctions supporting cell adhesion and, alternatively, as a nonredundant mediator of canonical Wnt signaling. Stimulation by Wnt ligands prevents cytoplasmic β-catenin degradation, which in turn allows its nuclear translocation and interaction with the transcription factor T cell factor 4 (TCF4, also known as Tcf7l2) to induce transcription of β-catenin target genes (*21*). These distinct adhesive and signaling activities of β-catenin stem from its structure: For adhesive function, central Armadillo repeats are essential, while N- and C-terminal domains are dispensable (*21*, *22*). β-Catenin signaling activity, on the other hand, requires the Armadillo repeats plus N- and/or C-terminal domains (*21*, *22*).

We also identified an essential role for the β-catenin C-terminal domain in SMCs for arterial wall assembly during embryogenesis, a

[1]Department of Medicine (Cardiology Division), Department of Developmental and Molecular Biology, and Wilf Family Cardiovascular Research Institute, Albert Einstein College of Medicine, Bronx, NY, USA. [2]Department of Pharmacology, Ribeirao Preto Medical School, University of Sao Paulo, Ribeirao Preto, SP, Brazil. [3]Institute of Molecular Life Sciences, University of Zurich, Zurich, Switzerland. [4]Vascular Biology Program, Boston Children's Hospital, Department of Surgery, Harvard Medical School, Boston, MA, USA.
*Corresponding author. Email: nicholas.sibinga@einsteinmed.edu (N.E.S.S.); dario.riascosbernal@einsteinmed.edu (D.F.R.-B.)

process for which the Armadillo repeats and N-terminal domain were not sufficient (*23*). In adulthood, expression of β-catenin is induced after vascular injury (*19*, *24*, *25*). Reduction of Wnt signaling activity (*26*), elimination of cells in which Wnt/β-catenin is activated after injury (*27*), and inactivation of β-catenin itself in SMCs (*19*) are sufficient to limit injury-induced neointimal thickening. Whether this essential function in vascular remodeling depends specifically on β-catenin C-terminal signaling is unknown. Given that SMC phenotype during vascular remodeling resembles a developmental phenotype (*28*), we hypothesized that signaling mediated by the β-catenin C terminus is required for arterial occlusion after injury and, therefore, that inhibitors of β-catenin C-terminal signaling (*29*, *30*) might limit neointima formation after injury and atherosclerotic lesion expansion.

The focus of the present study was to investigate the importance of SMC β-catenin C-terminal signaling for vascular remodeling in adulthood and the underlying molecular mechanisms. To this end, we used a tamoxifen-inducible and tissue-specific genetic approach in the mouse to inactivate SMC β-catenin C-terminal signaling in adulthood. We show that the β-catenin C-terminal domain is essential in vivo for neointima formation after arterial injury. Further studies provide evidence that β-catenin interacts with the *S1pr1* promoter and acts through its C-terminal domain to activate *S1pr1* transcription and protein expression, ultimately enhancing SMC proliferation. We also show that arteries from mice lacking the β-catenin C terminus in SMCs exhibit lower S1PR1 protein expression and neointima formation after injury, and, notably, that restoring the expression of S1PR1 in SMCs in vivo increases neointima formation in β-catenin C terminus–deficient mice toward control levels. Last, our pharmacological approach shows that E7386, an inhibitor of the β-catenin C terminus, inhibits S1PR1 expression, neointima formation after arterial injury, and atherosclerosis development. Collectively, these findings identify β-catenin C-terminal output as an upstream regulator of S1PR1 expression and define a functional interaction between the canonical Wnt and S1P signaling pathways that drives arterial occlusion.

RESULTS

SMC β-catenin C-terminal signaling is required for neointima formation after vascular injury

To test whether the β-catenin C-terminal domain is required in SMCs for vascular remodeling, we studied mice bearing a validated mutant β-catenin allele (*31*) encoding a truncated β-catenin protein (ΔC) that is incapable of interaction with multiple transcriptional coactivators. Expression of β-catenin in SMCs is necessary for embryonic development (*23*), so to mediate temporal and conditional inactivation of β-catenin expression selectively in SMCs, we used the tamoxifen-inducible *Acta2-CreER*^{T2} driver line (*32*). For lineage tracing, we added a Cre-activated fluorescent reporter [red fluorescent protein (RFP), also referred as TdTomato] transgene in the *Rosa26* locus (*33*). Our breeding strategy generated mice bearing one β-catenin flox allele and either one knockin mutant (*Ctnnb1*$^{\Delta C/flox}$) or wild-type (WT) (*Ctnnb1*$^{WT/flox}$; control) β-catenin allele, both carrying the *Acta2-CreER*^{T2} and RFP transgenes. In this system, tamoxifen administration removes the β-catenin flox allele, resulting in mice expressing either the mutant allele (designated as SMβC$^{\Delta C}$ mice) or the WT allele (designated as SMβC$^{WT/-}$ mice) as the only source of β-catenin protein in SMCs (Fig. 1A and Table 1). In addition, tamoxifen administration activates RFP for SMC lineage tracing. Taking advantage of the lineage tracing system, we found that all RFP$^+$ cells in noninjured carotid arteries from both SMβC$^{\Delta C}$ and SMβC$^{WT/-}$ mice are also positive for smooth muscle α-actin (SMA) and are restricted to the medial layer of the vessel (fig. S1A), suggesting that, at least in the vascular wall, *Acta2-CreER*^{T2} is selectively activated in SMCs but not in other cell types. As an additional control, we stained noninjured carotid arteries from both SMβC$^{\Delta C}$ and SMβC$^{WT/-}$ mice that did not receive tamoxifen for RFP and SMA and found clear signals for SMA, but no signals for RFP (fig. S1B), indicating that autofluorescence and Cre-independent RFP expression are not relevant factors.

Western analysis of aortic lysates using an antibody against the β-catenin C terminus showed marked reduction of the β-catenin band, whereas an antibody against the β-catenin N terminus yielded an 80-kDa band (apparent molecular weight consistent with the loss of the C terminus) (Fig. 1, B and C). Immunofluorescent studies with the anti–β-catenin N-terminal antibody showed a positive signal in RFP$^+$ cells in carotid arteries of both SMβC$^{WT/-}$ and SMβC$^{\Delta C}$ mice, while the anti–C-terminal antibody signal was lost in the latter (fig. S2, A and C). Neither anti–N-terminal nor anti–C-terminal antibodies showed signals for β-catenin in RFP$^+$ cells in carotid arteries of smooth muscle β-catenin knockout (SMβC$^{-/-}$) mice, included as negative control (fig. S2B). In addition, we evaluated the expression of Axin2, a typical target of β-catenin signaling (*34*), and found that Axin2 expression was highly induced in RFP$^+$ cells from carotid arteries of SMβC$^{WT/-}$ mice after injury but markedly lower in injured arteries from SMβC$^{\Delta C}$ mice (fig. S2, D and E). These findings validate effective, SMC-selective genetic inactivation of β-catenin C-terminal signaling.

Then, we asked whether complete or C terminus–specific β-catenin inactivation in SMCs in adulthood affected overall health or vascular homeostasis of unchallenged mice. We followed blood pressure and body weight of male and female SMβC$^{WT/-}$, SMβC$^{\Delta C}$, and SMβC$^{-/-}$ mice from just before the first tamoxifen administration until 12 weeks after the last tamoxifen injection. We observed normotensive blood pressures, no lethality or morbidity, and no change in body weight gain, regardless of sex or time point, in any of the groups (fig. S3, A and B). Similarly, the structure of uninjured aorta and carotid arteries harvested at the 12-week time point appeared unchanged (fig. S4, A and B). These findings suggest that full-length or C-terminal domain β-catenin functions are not required—at least for 3 months—for overall health maintenance and vascular homeostasis of unchallenged mice.

We then assessed the importance of SMC β-catenin C-terminal signaling in the response to vascular injury, which has not been previously evaluated. To induce such an injury, we performed carotid artery ligation 1 week after the first tamoxifen injection in male and female SMβC$^{\Delta C}$ and littermate control (SMβC$^{WT/-}$) mice and harvested ligated and uninjured arteries at 21 days after surgery. Both male and female SMβC$^{\Delta C}$ mice exhibited marked decreases in neointima formation after injury compared to SMβC$^{WT/-}$ mice (Fig. 1D). We noted reduced intima area (Fig. 1F) and decreased intima/media ratio (Fig. 1G) in SMβC$^{\Delta C}$ mice of both sexes, with no differences in medial area (Fig. 1E). We also found that expression of CD31, an endothelial marker, is limited to the layer of cells outlining the lumen of the vessel, while other cells forming the neointima express RFP in both SMβC$^{WT/-}$ and SMβC$^{\Delta C}$ mice (fig. S5), indicating that SMCs and their derivatives are the main contributors to neointimal expansion.

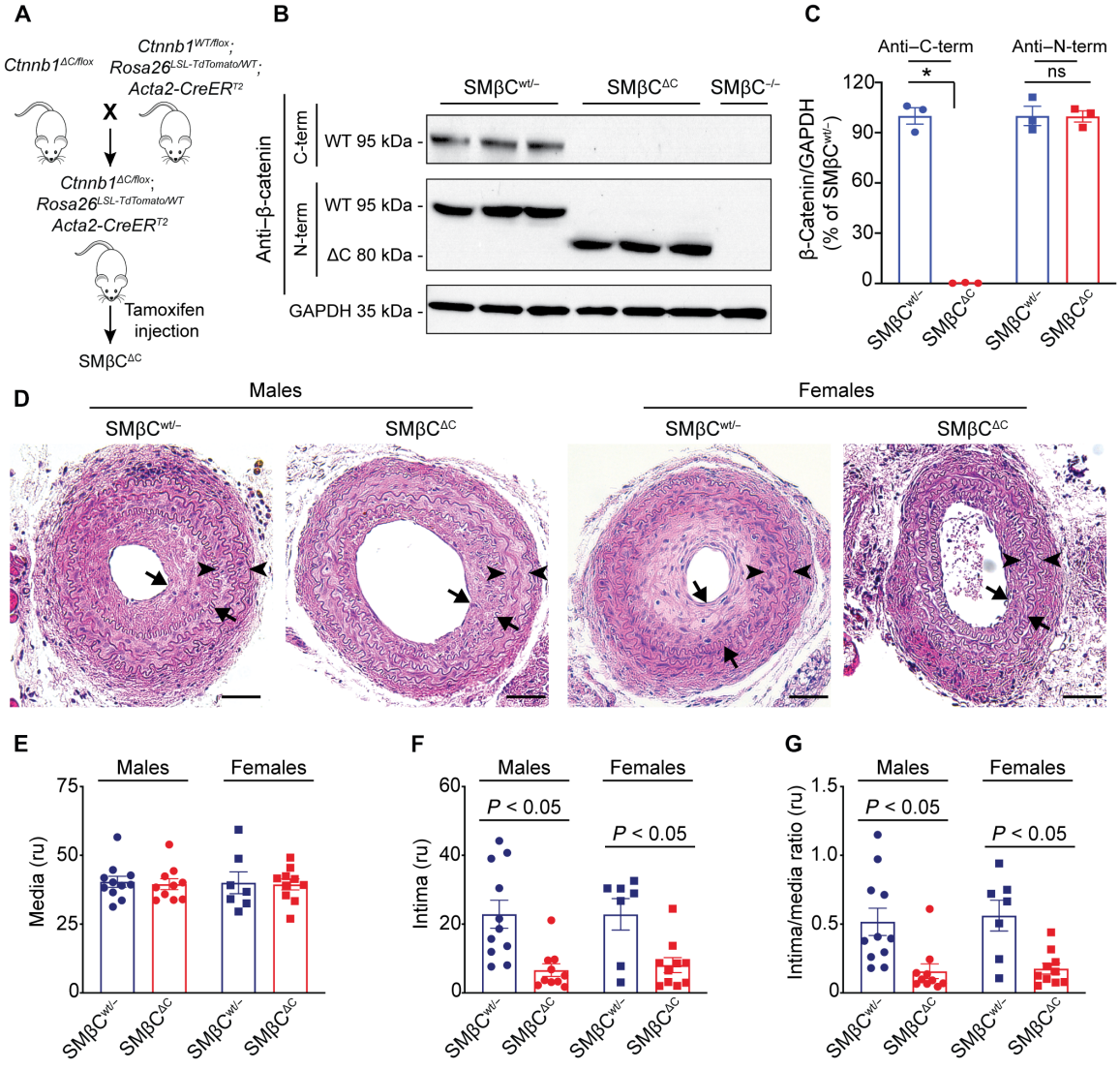

Fig. 1. Smooth muscle β-catenin C-terminal signaling promotes neointima formation after carotid artery ligation. (**A**) Schematic representation of the breeding strategy to obtain smooth muscle β-catenin C terminus–deficient (SMβC$^{\Delta C}$) mice. *Ctnnb1*$^{WT/flox}$;*Rosa26*$^{LSL\text{-}TdTomato/WT}$;*Acta2-CreER*^{T2} mice were generated from the same breeders. (**B**) Representative Western blotting for β-catenin in total arterial protein lysates isolated from aortas of WT (SMβC$^{WT/-}$), smooth muscle β-catenin C terminus–deficient (SMβC$^{\Delta C}$), and smooth muscle β-catenin knockout (SMβC$^{-/-}$) mice after tamoxifen injection. Different β-catenin antibodies targeting the C- or N-terminal domains (C-term or N-term, respectively) of the protein were used. Arterial lysates from smooth muscle β-catenin knockout (SMβC$^{-/-}$) mice were used as a negative control. (**C**) Densitometric analysis of β-catenin protein levels evaluated by using distinct antibodies targeting the C- or N-terminal domain of the protein, normalized to GAPDH ($n = 3$). Statistical analysis: Unpaired Student's *t* test. *$P < 0.05$. Data are means ± SEM of independent biological replicates. (**D**) Representative images of H&E-stained carotid arteries 21 days after ligation. Arrows delimit the neointimal layer, while arrowheads indicate the medial layer. Scale bars, 50 μm. (**E** to **G**) Morphometric measurements of the medial area (E), intimal area (F), and a ratio of intimal to medial area (G). Each dot represents a single mouse. Statistical analysis: Unpaired Student's *t* test. Values are represented as means ± SEM of independent biological replicates. $n = 11$ for SMβC$^{WT/-}$ males, $n = 7$ for SMβC$^{WT/-}$ females, and $n = 10$ for SMβC$^{\Delta C}$ males and females.

These observations indicate that β-catenin C-terminal signaling is required in SMCs for neointima formation after injury in adulthood.

Loss of SMC β-catenin C-terminal signaling in vivo reduces cell proliferation and dedifferentiation but increases apoptosis

Reduced neointimal formation in SMβC$^{\Delta C}$ mice could be due to decreased SMC proliferation and/or increased apoptosis, so we evaluated expression of the proliferating cell nuclear antigen (PCNA) or Ki67, markers of cell proliferation, and cleaved caspase-3, a marker of apoptosis, in injured carotid artery sections. We found reduced percentages of PCNA$^+$ or Ki67$^+$ SMC nuclei in the neointima and media area of arteries from SMβC$^{\Delta C}$ mice compared to SMβC$^{WT/-}$ mice (Fig. 2, A and B, and fig. S6, A to D).

On the other hand, we observed an increased percentage of SMCs positive for cleaved caspase-3 in the neointima and media areas of arteries from SMβC$^{\Delta C}$ mice compared to SMβC$^{WT/-}$ mice (Fig. 2, C and D). Decreased expression of SMC differentiation

Table 1. Summary of transgenic mouse groups used in the study.

Genotype	Abbreviation	β-Catenin protein expressed in SMCs after tamoxifen	Functions in SMCs after tamoxifen
Ctnnb1$^{WT/flox}$;*Rosa26*$^{LSL\text{-}TdTomato/WT}$;*Acta2-CreER*^{T2}	SMβC$^{WT/-}$	WT	β-Catenin control (WT); lineage tracing
Ctnnb1$^{\Delta C/flox}$;*Rosa26*$^{LSL\text{-}TdTomato/WT}$;*Acta2-CreER*^{T2}	SMβC$^{\Delta C}$	Only β-catenin$^{\Delta C}$	No β-catenin C-terminal signal; lineage tracing
Ctnnb1$^{flox/flox}$;*Rosa26*$^{LSL\text{-}TdTomato/WT}$;*Acta2-CreER*^{T2}	SMβC$^{-/-}$	None	β-Catenin knockout; lineage tracing
Ctnnb1$^{WT/flox}$ *Rosa26*$^{LSL\text{-}TdTomato/LSL\text{-}S1pr1}$;*Acta2-CreER*^{T2}	SMβC$^{WT/-}$ SM-S1PR1^{GOF}	WT	GOF of S1PR1; lineage tracing
Ctnnb1$^{\Delta C/flox}$;*Rosa26*$^{LSL\text{-}TdTomato/LSL\text{-}S1pr1}$;*Acta2-CreER*^{T2}	SMβC$^{\Delta C}$ SM-S1PR1^{GOF}	Only β-catenin$^{\Delta C}$	No β-catenin C-terminal signal; GOF of S1PR1; lineage tracing

markers is another hallmark of vascular remodeling (*2*), so we wondered whether this process is affected by loss of SMC β-catenin C-terminal function. Arterial injury decreased levels of the SMA differentiation marker in RFP$^+$ cells of ligated carotid arteries from SMβC$^{WT/-}$ mice (Fig. 2, E and F, and fig. S7) but not in those of SMβC$^{\Delta C}$ mice (Fig. 2, E and F, and fig. S7). Together, these findings support the idea that the proproliferative, prosurvival, and dedifferentiation functions of β-catenin in SMCs during vascular remodeling are mediated through its C terminus.

Inhibition of SMC β-catenin C-terminal signaling down-regulates S1PR1 expression

To gain mechanistic insights, we isolated mouse aortic SMCs (MASMCs) from *Ctnnb1*$^{\Delta C/flox}$ mice and transduced them with green fluorescent protein (GFP)–expressing or Cre-expressing adenovirus to generate control (βC^{Control}) or β-catenin C terminus–deficient (βC$^{\Delta C}$) cells, respectively. Western analysis using antibodies against the β-catenin C- and N-terminal domains confirmed that C terminus–deficient β-catenin is the only form of this protein expressed in βC$^{\Delta C}$ MASMCs (Fig. 3A). Then, we characterized the phenotype of βC^{Control} and βC$^{\Delta C}$ MASMCs by evaluating cell population growth and found that MASMCs bearing βC$^{\Delta C}$ as the only form of β-catenin showed reduced growth compared to βC^{Control} cells (Fig. 3B).

To explore the potential downstream molecular mechanisms underlying the effects of β-catenin C-terminal signaling in SMCs, we performed RNA-sequencing (RNA-seq) analysis. Principal components analysis (PCA) of transcriptomes from βC^{Control} and βC$^{\Delta C}$ MASMCs appeared distinct (Fig. 3C), with the latter showing up-regulation of 1518 genes and down-regulation of 1925 genes compared with control (Fig. 3D). Evaluation on the Ingenuity Pathway Analysis (IPA) platform identified significant down-regulation in βC$^{\Delta C}$ cells of canonical signaling pathways associated with proproliferative, prosurvival and dedifferentiated phenotypes, such as "cardiac hypertrophy signaling," "wound healing signaling," "signal transducer and activator of transcription 3 (STAT3) pathway," "extracellular signal–regulated kinase/mitogen-activated protein kinase (MAPK) signaling," and "PTEN signaling" (Fig. 3E). Both the broad "GPCR signaling" category and the more specific subset of "S1P signaling" were also identified. Closer examination of S1P-related transcripts revealed decreased *S1pr1* and *S1pr3* levels, with little change for *S1pr2*, *S1pr5*, and *Sphk1* and *Sphk2* (the last two encoding sphingosine kinase 1 and 2, respectively) (Fig. 3F). By quantitative reverse transcription polymerase chain reaction (qPCR), we confirmed the decrease in *S1pr1* mRNA levels in βC$^{\Delta C}$ MASMCs compared to βC^{Control} (Fig. 3G); this finding is reminiscent of a previous study in which we found decreased *S1pr1* levels in SMCs lacking full-length β-catenin (*19*). On the other hand, both qPCR for *S1pr3* (Fig. 3G) and Western blotting for S1PR3 protein (fig. S8) showed no difference in expression. Together, these findings suggest that loss of β-catenin C-terminal signaling in SMCs reduces cell growth and down-regulates *S1pr1* expression, the latter effect with some selectivity within the S1P pathway.

S1PR1 is a β-catenin transcriptional target that mediates β-catenin–induced cell population growth in MASMCs

Decreased expression of *S1pr1* in β-catenin C terminus–deficient MASMCs is consistent with a previous study in which we found lower *S1pr1* transcript levels in MASMCs lacking full-length β-catenin (*19*). To extend this observation, we performed Western analysis, which showed reduced S1PR1 protein expression in βC$^{\Delta C}$ MASMCs compared to βC^{Control} (Fig. 4A). The decreased S1PR1 expression observed in βC$^{\Delta C}$ MASMCs was restored when these cells were transfected with β-catenin^{S33Y}, a full-length, constitutively active form of β-catenin (Fig. 4B). In addition, treatment with CHIR99021, a small molecule that prevents β-catenin degradation, increased S1PR1 expression in a dose-dependent manner in βC^{Control} MASMCs, but did not affect S1PR1 expression in βC$^{\Delta C}$ MASMCs (Fig. 4C), suggesting that the β-catenin C-terminal domain is essential for S1PR1 expression in SMCs.

The upstream factors that control S1PR1 expression in SMCs are not fully understood, so we investigated potential molecular mechanisms. To test whether the β-catenin C-terminal domain is required for *S1pr1* promoter activation, βC^{Control} and βC$^{\Delta C}$ MASMCs were transfected with a validated human *S1PR1* promoter–driven luciferase reporter (*35*). Loss of β-catenin C-terminal signaling markedly reduced *S1PR1* promoter activity, which recovered with cotransfection of a plasmid encoding β-catenin^{S33Y} (Fig. 4D). We further investigated whether *S1pr1* is a direct β-catenin transcriptional target. β-Catenin lacks a DNA binding domain, and it partners with TCF4 to interact with target genes (*21*). To examine whether β-catenin and/or TCF4 bind to the *S1pr1* promoter in MASMCs, we performed a CUT&RUN (cleavage under targets and release using nuclease) assay using anti–β-catenin and anti-TCF4 antibodies, plus

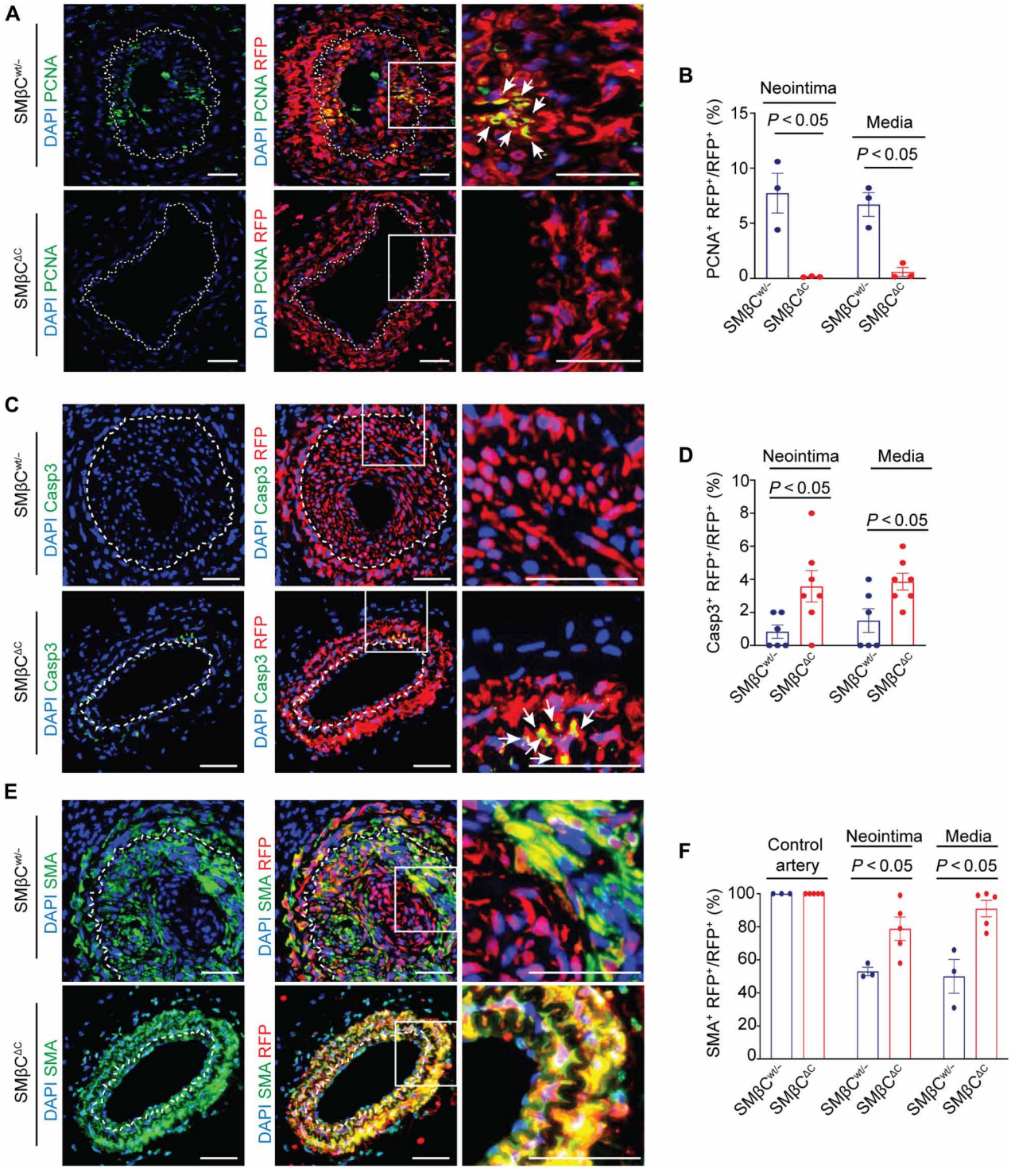

Fig. 2. Loss of SMC β-catenin C-terminal signaling decreases SMC proliferation and dedifferentiation and increases apoptosis. (**A**) Immunostaining for PCNA, a marker of proliferation, and RFP, SMC lineage tracer, in carotid arteries 21 days after ligation. Dotted line marks the internal elastic lamina (IEL). Scale bar, 50 μm. (**B**) Percentage of SMCs positive for PCNA. Only nuclear signals were included in the quantification. Statistical analysis: Unpaired Student's *t* test. $n = 3$. Data are means ± SEM of independent biological replicates. (**C**) Immunostaining for cleaved caspase-3 (Casp3), a marker of apoptosis, and RFP in carotid arteries 21 days after ligation. Dotted line marks the IEL. Scale bar, 50 μm. (**D**) Percentage of SMCs positive for cleaved caspase-3. Statistical analysis: Unpaired Student's *t* test. $n = 6$ for SMβC$^{WT/-}$ and $n = 7$ for SMβC$^{\Delta C}$. Data are means ± SEM of independent biological replicates. (**E**) Immunostaining for SMA and RFP in carotid arteries 21 days after ligation. Dotted line marks the IEL. Scale bar, 50 μm. (**F**) Percentage of SMCs positive for SMA in uninjured (control) and ligated carotid arteries. Statistical analysis: Unpaired Student's *t* test. $n = 3$ for SMβC$^{WT/-}$ and $n = 5$ for SMβC$^{\Delta C}$. Data are means ± SEM of independent biological replicates.

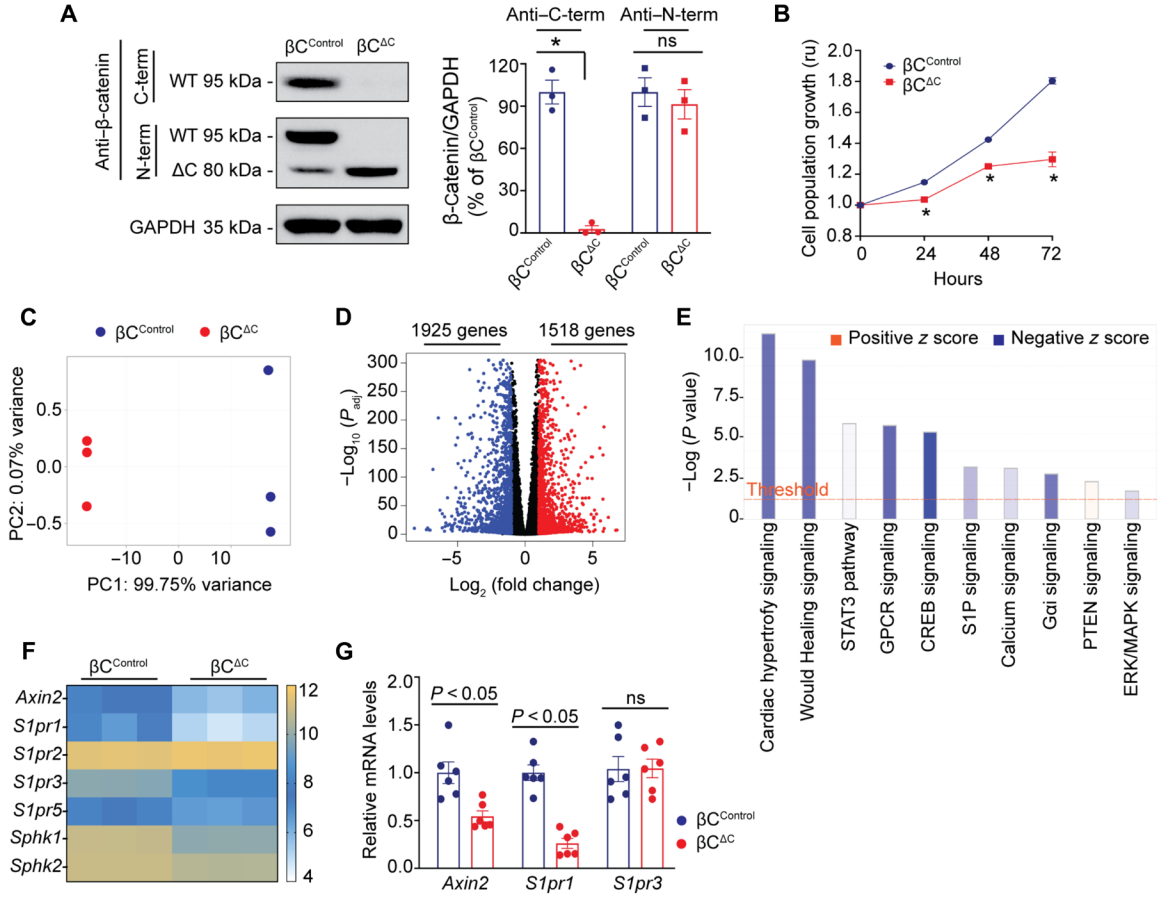

Fig. 3. Loss of SMC β-catenin C-terminal signaling reduces SMC growth and down-regulates *S1pr1* expression. (**A**) Western blotting for β-catenin in $\beta C^{Control}$ and $\beta C^{\Delta C}$ MASMCs. Different antibodies targeting the C- or N-terminal domains (C-term or N-term, respectively) of β-catenin were used. *$P < 0.05$, unpaired Student's *t* test. $n = 3$. ns, not significant. Data are means ± SEM of independent biological replicates. (**B**) Cell population growth of $\beta C^{Control}$ and $\beta C^{\Delta C}$ MASMCs. *$P < 0.05$, two-way ANOVA with Šídák's multiple comparison test. $n = 6$. Data are means ± SEM of independent biological replicates. (**C**) PCA from RNA-seq of $\beta C^{Control}$ and $\beta C^{\Delta C}$ MASMCs. Each dot represents an independent sample. (**D**) Volcano plot. Each data point represents a gene. The $\log_2$ fold change of each gene is represented on the *x* axis, and the $\log_{10}$ of its adjusted *P* value (P_{adj}) is on the *y* axis. Red dots indicate significantly up-regulated genes ($\log_2$ fold change > 1 and $P_{adj} < 0.05$), while blue dots represent significantly down-regulated genes ($\log_2$ fold change < −1 and $P_{adj} < 0.05$) in $\beta C^{\Delta C}$ MASMCs compared to $\beta C^{Control}$. The black dots represent genes that do not satisfy the above conditions. (**E**) Significantly enriched canonical signaling pathways identified by IPA and ranked by *P* value. Positive and negative *z* scores indicate up- and down-regulated signaling pathways, respectively, in $\beta C^{\Delta C}$ versus $\beta C^{Control}$ MASMCs. (**F**) Heatmap derived from the RNA-seq data, showing the relative expression (color scale on the right) of *Axin2*, a known β-catenin target gene, and key components of the S1P signaling pathway in $\beta C^{Control}$ and $\beta C^{\Delta C}$ MASMCs. (**G**) qPCR for *Axin2*, *S1pr1*, and *S1pr3*, which were significantly down-regulated in $\beta C^{\Delta C}$ MASMCs in RNA-seq analysis. *Rpl13* and *β-actin* were used as housekeeping controls. Statistical analysis: Unpaired Student's *t* test. $n = 6$. Data are means ± SEM of independent biological replicates.

qPCR to amplify different regions of the *S1pr1* promoter. This assay revealed recruitment of β-catenin and TCF4 to a region of the *S1pr1* promoter containing a consensus TCF binding motif, 5′-TCAAAG (fragment −939/−790; Fig. 4E). Such recruitment was not observed in other regions of the *S1pr1* promoter that lack a consensus TCF binding motif (fragments −1973/−1802 and −638/−512; Fig. 4E). In addition, we found that in serum-deprived, quiescent MASMCs, β-catenin is not recruited to the *S1pr1* promoter (fig. S9, A and B), consistent with reduced β-catenin and S1PR1 expression in these conditions (fig. S9C). Together, these findings show that under stimulated but not quiescent conditions, β-catenin and TCF4 bind to the *S1pr1* promoter in SMCs, activating expression of S1PR1 through a β-catenin C terminus–dependent function.

We then characterized how decreased S1PR1 expression contributes to the $\beta C^{\Delta C}$ SMC phenotype. We isolated MASMCs from *Ctnnb1*$^{\Delta C/flox}$ mice also bearing a Cre-conditional S1PR1 gain-of-function (GOF) allele (*36*) and transduced the cells with GFP or Cre-expressing adenovirus to generate control ($\beta C^{Control}$ $S1PR1^{Control}$) or $\beta C^{\Delta C}$ cells with restored S1PR1 ($\beta C^{\Delta C}$ $S1PR1^{GOF}$), respectively. Western blotting validated the technical strategy (fig. S10). Expression of S1PR1 in β-catenin C terminus–deficient MASMCs ($\beta C^{\Delta C}$ $S1PR1^{GOF}$) restored cell growth toward control levels (Fig. 4F), thereby suppressing the growth phenotype observed in C terminus–deficient MASMCs. In complementary studies, we induced β-catenin GOF in MASMCs with CHIR99021 and knocked down S1PR1 using a small interfering RNA (siRNA) (fig. S11A). Loss of S1PR1 prevented the increase in cell growth promoted by CHIR99021 (fig. S11B), showing that S1PR1 is required for the increased SMC growth induced by β-catenin gain of function. Together, these observations are consistent with the idea that *S1pr1* is a critical target gene for

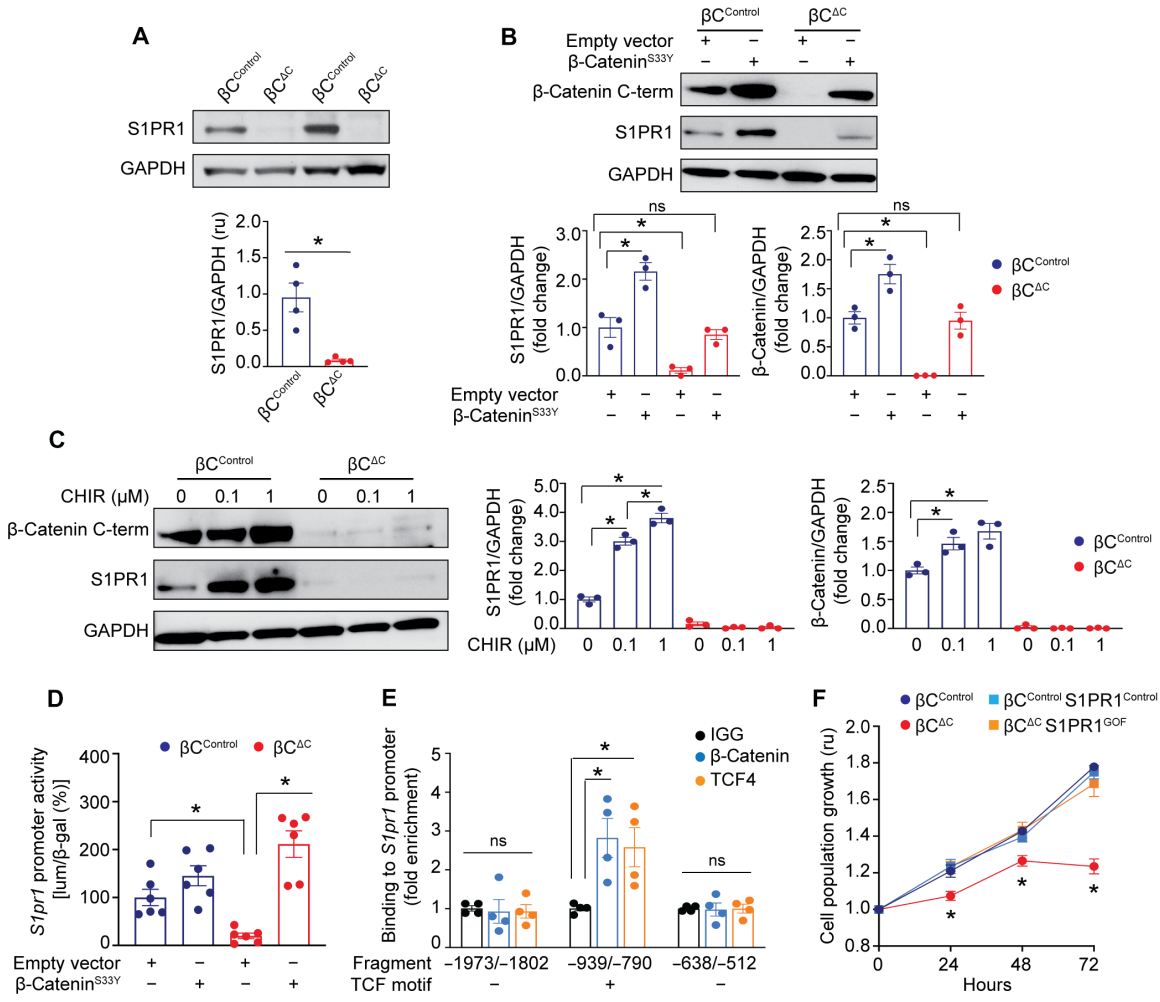

Fig. 4. S1PR1 is a transcriptional target of β-catenin and rescues the defective growth of βC$^{\Delta C}$ MASMCs toward control levels. (**A**) Representative Western blotting and densitometric analysis of S1PR1 in βC^{Control} and βC$^{\Delta C}$ MASMCs, normalized to GAPDH. *$P < 0.05$, unpaired Student's t test. $n = 4$. (**B**) Representative Western blotting and densitometric analysis of S1PR1 and β-catenin in βC^{Control} and βC$^{\Delta C}$ MASMCs electroporated with empty vector or β-catenin^{S33Y}, a constitutively active form of β-catenin. *$P < 0.05$, two-way ANOVA with Šídák's multiple comparison test. $n = 3$. (**C**) Representative Western blotting and densitometric analysis of S1PR1 and β-catenin in βC^{Control} and βC$^{\Delta C}$ MASMCs treated with CHIR99021 (CHIR), a small molecule that prevents β-catenin degradation. *$P < 0.05$, one-way ANOVA with Tukey's multiple comparison test. $n = 3$. (**D**) βC^{Control} and βC$^{\Delta C}$ MASMCs were co-electroporated with a human *S1PR1*-driven luciferase reporter (pGL3-*S1PR1*-promoter) and empty vector or β-catenin^{S33Y}. Forty-eight hours after transfection, cells were harvested for luciferase assay. Luminescence (lum) was normalized to β-galactosidase activity (β-gal) to control for transfection efficiency and expressed relative to empty vector in βC^{Control} MASMCs. *$P < 0.05$, two-way ANOVA with Šídák's multiple comparison test. $N = 6$. (**E**) CUT&RUN assay was conducted in MASMCs using anti–β-catenin, anti-TCF4, and anti-IgG antibodies and analyzed by qPCR using primers that amplify different regions in the *S1pr1* promoter containing (+) or not (−) a consensus TCF binding motif, 5′-TCAAAG. Indicated locations are relative to transcription start site. *$P < 0.05$, unpaired Student's t test. $N = 4$. (**F**) Cell population growth of βC^{Control}, βC$^{\Delta C}$, βC^{Control} S1PR1^{GOF}, and βC$^{\Delta C}$ S1PR1^{GOF} MASMCs. *$P < 0.05$ compared to other groups, two-way ANOVA with Šídák's multiple comparison test. $n = 6$. Data shown in (A) to (F) are means ± SEM of independent biological replicates.

β-catenin C-terminal signaling that drives proliferation of SMCs in culture.

β-Catenin C-terminal signaling promotes neointima formation after vascular injury by inducing S1PR1 expression in SMCs

To test the in vivo relevance of the above findings, we first examined S1PR1 expression in control and ligated carotid arteries from SMβC$^{\Delta C}$ and SMβC$^{WT/-}$ mice. We found a clear signal for S1PR1 in the endothelial layer but could not detect S1PR1 expression in SMCs of control, uninjured arteries from either SMβC$^{\Delta C}$ or SMβC$^{WT/-}$ mice (fig. S12). On the other hand, we found a high percentage of S1PR1^{+} SMCs in injured arteries from SMβC$^{WT/-}$ mice, which was decreased in injured arteries from SMβC$^{\Delta C}$ mice (Fig. 5, A and B). Because we found that loss of β-catenin C-terminal domain in SMCs reduced neointima formation after vascular injury (Fig. 1, D and G) and this effect was associated with reduced S1PR1 expression (Fig. 5, A and B), we wondered whether restoring S1PR1 expression in SMβC$^{\Delta C}$ mice could reestablish injury-induced neointima formation. To test this idea, we crossed the Cre-conditional S1PR1 GOF mouse line (*Rosa26*$^{LSL\text{-}S1pr1}$) (*36*) with *Ctnnb1*$^{\Delta C/flox}$;*Acta2-CreER*^{T2} or *Ctnnb1*$^{WT/flox}$;*Acta2-CreER*^{T2} mice to generate mice that upon tamoxifen administration express in SMCs a

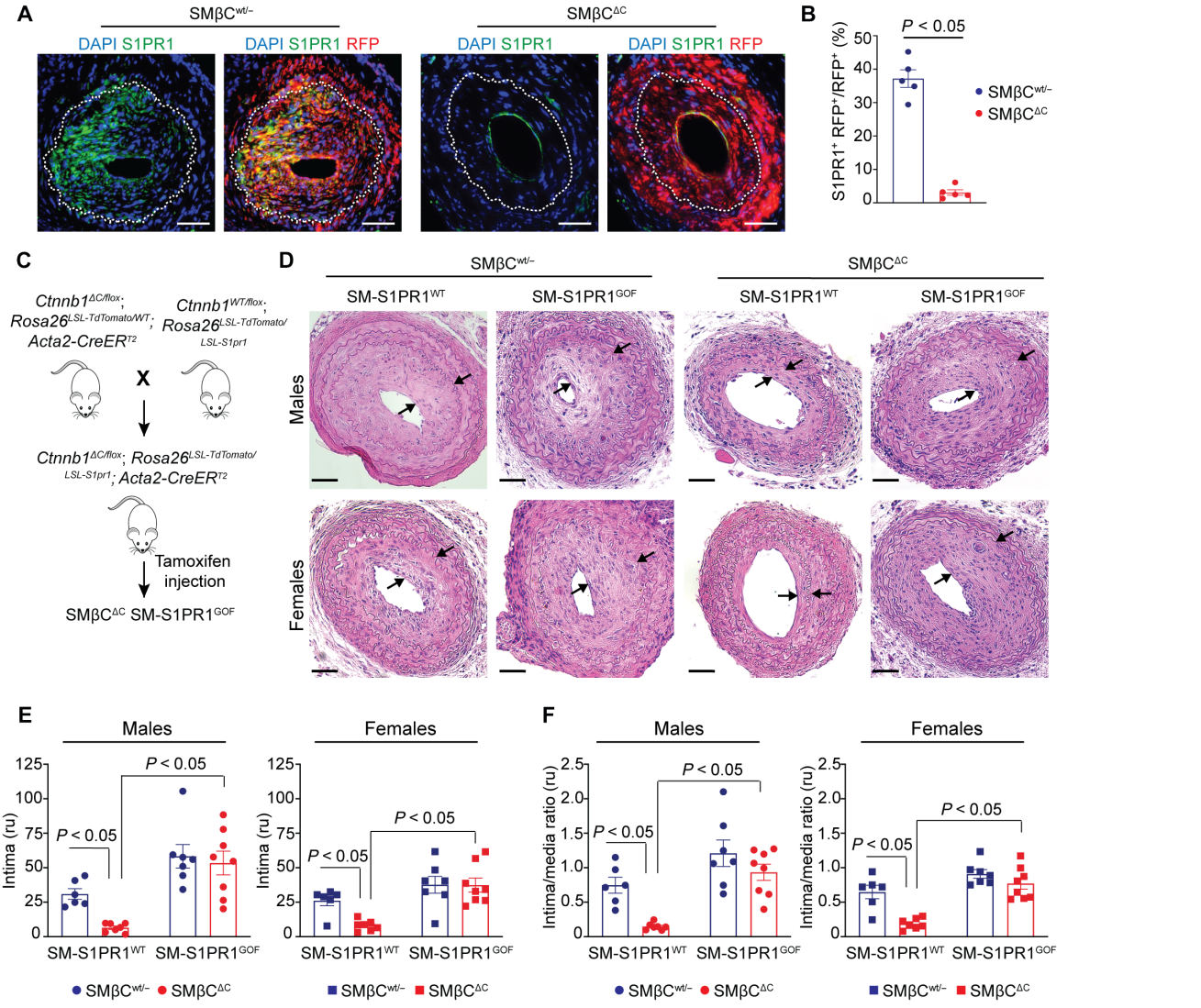

Fig. 5. Reestablishing S1PR1 expression in SMCs rescues injury-induced neointima formation in β-catenin C terminus–deficient mice. (**A**) Immunostaining for S1PR1 and RFP in carotid arteries 21 days after ligation. Dotted line marks the IEL. Scale bars, 75 μm. (**B**) Percentage of SMCs positive for S1PR1 in the media and neointima area of carotid arteries. Statistical analysis: Unpaired Student's *t* test. $n = 5$. Data are means ± SEM of independent biological replicates. (**C**) Schematic representation of the breeding strategy to obtain smooth muscle–specific β-catenin C terminus–deficient mice with a GOF for S1PR1 (SMβC$^{\Delta C}$ SM-S1PR1^{GOF}) mice. *Ctnnb1*$^{WT/flox}$; *Rosa26*$^{LSL\text{-}TdTomato/LSL\text{-}S1pr1}$;*Acta2-CreER*^{T2} mice were generated from the same breeders. (**D**) Representative images of H&E-stained carotid arteries from SMβC$^{WT/-}$, SMβC$^{\Delta C}$, SMβC$^{WT/-}$ SM-S1PR1^{GOF}, and SMβC$^{\Delta C}$ SM-S1PR1^{GOF} mice, 21 days after ligation. Arrows delimit the neointimal growth. Scale bars, 75 μm. (**E** and **F**) Morphometric measurements of the intimal area (E) and a ratio of intimal to medial area (F). Each dot represents a single mouse. Statistical analysis: Two-way ANOVA with Šídák's multiple comparison test. $n = 6$ for SMβC$^{WT/-}$ males and females, $n = 7$ for SMβC$^{\Delta C}$ males and females, $n = 7$ for SMβC$^{WT/-}$ SM-S1PR1^{GOF} males and females, and $n = 8$ for SMβC$^{\Delta C}$ SM-S1PR1^{GOF} males and females. Values are represented as means ± SEM of independent biological replicates.

GOF S1PR1 allele and the C terminus–deficient β-catenin allele (designated as SMβC$^{\Delta C}$ SM-S1PR1^{GOF} mice) or a GOF S1PR1 allele and a WT β-catenin allele (designated as SMβC$^{WT/-}$ SM-S1PR1^{GOF} mice) (Fig. 5C and Table 1). Susceptibility to neointima formation was studied at 21 days after ligation of carotid arteries in the following four different groups: SMβC$^{WT/-}$ SM-S1PR1^{GOF}, SMβC$^{\Delta C}$ SM-S1PR1^{GOF}, SMβC$^{WT/-}$, and SMβC$^{\Delta C}$ mice. Increased expression of S1PR1 in SMCs within ligated carotid arteries of SMβC$^{WT/-}$ SM-S1PR1^{GOF} and SMβC$^{\Delta C}$ SM-S1PR1^{GOF} mice was confirmed by immunofluorescence (fig. S13). We observed greater neointima formation in both male and female SMβC$^{\Delta C}$ SM-S1PR1^{GOF} mice compared to SMβC$^{\Delta C}$ mice (Fig. 5D). In particular, we found increased intima area (Fig. 5E) and a higher intima/media ratio (Fig. 5F) in male and female SMβC$^{\Delta C}$ SM-S1PR1^{GOF} mice compared to SMβC$^{\Delta C}$ mice, with no differences in medial area (fig. S14). No difference in neointima size was observed between SMβC$^{\Delta C}$ SM-S1PR1^{GOF} mice and SMβC$^{WT/-}$ mice (Fig. 5, D to F). These findings show that restoring expression of S1PR1 in SMCs reestablishes neointima formation in mice lacking the β-catenin C-terminal domain in SMCs. Together, these data are consistent with the idea that signaling mediated by the C-terminal domain of β-catenin in SMCs is essential for vascular remodeling after injury, in part by inducing S1PR1 expression and function.

Pharmacologic inhibition of β-catenin C-terminal signaling decreases S1PR1 expression in SMCs, attenuates neointimal formation, and limits atherosclerosis

The above findings derived from our genetic strategies provide a solid rationale to assess the effects of pharmacological inhibition of β-catenin C-terminal signaling on vascular remodeling. To investigate such effects, we used E7386, a first-in-class orally active β-catenin C-terminal inhibitor that has been reported to inhibit the binding of the β-catenin C terminus to Creb-binding protein (CBP), a transcriptional coactivator, and to reduce canonical Wnt signaling–dependent gene expression (*29*). To confirm the specificity of E7386 for the C-terminal domain of β-catenin, we compared its effects on $\beta C^{Control}$ and $\beta C^{\Delta C}$ MASMCs. We found that E7386 at 10 to 100 nM decreased cell growth of $\beta C^{Control}$ MASMCs (Fig. 6A and fig. S15, A and B). The magnitude of growth inhibition in $\beta C^{Control}$ MASMCs treated with 100 nM E7386 was similar to that observed in MASMCs lacking the β-catenin C terminus ($\beta C^{\Delta C}$ MASMC vehicle group; Fig. 6A), while E7386 at 50 and 10 nM yielded less pronounced but still significant inhibition (fig. S15, A and B). Notably, E7386 at 10 to 100 nM did not affect the cell growth of $\beta C^{\Delta C}$ MASMCs (Fig. 6A and fig. S15, A and B), indicating that the inhibitory effect of E7386 on SMC growth requires the β-catenin C terminus. In addition, MASMCs treated with E7386 exhibited reduced expression of Axin2 (fig. S15C), indicating that E7386 inhibits β-catenin C-terminal transcriptional activity. Consistent with this idea, E7386 also reduced S1PR1 expression in MASMCs (fig. S15C), because S1PR1 expression in these cells requires the β-catenin C-terminal transcriptional activity (Fig. 4). Together, these findings suggest that E7386 inhibits SMC proliferation by blocking interactions mediated by the β-catenin C terminus.

To test the in vivo relevance of the above findings, we induced vascular injury by carotid artery ligation in male and female WT C57BL/6J mice, followed by treatment with E7386 (50 mg/kg twice daily) by oral gavage for 14 days (Fig. 6B). Immunostaining for Axin2 shows reduced expression of this protein in SMA^+ cells of carotid arteries from mice treated with E7386, which is consistent with inhibition of β-catenin C-terminal signaling in SMCs in vivo (Fig. 6, C and D). We found that E7386 decreased the intimal area in females, trended toward a similar effect in males, and did not affect the media area in either sex (Fig. 6, E to G). Notably, in both females and males, E7386 reduced the intima/media ratio, a parameter of neointima formation that considers variation in blood vessel size (Fig. 6H). E7386 also reduced expression of S1PR1 in SMA^+ cells in the injured carotid arteries (Fig. 6, I and J). Together, these observations are consistent with the idea that pharmacological inhibition of the β-catenin C-terminal signaling decreases S1PR1 expression in SMCs and attenuates neointima formation after arterial injury.

These observations led us to test the effects of E7386 in a model of atherosclerosis, a highly prevalent and important disease in which SMCs play a critical role (*37*). To this end, we used a mouse model of disturbed flow–, hyperlipidemia-induced atherosclerosis (*38*), administering E7386 (25 mg/kg) or vehicle by oral gavage twice daily for 21 days after initiation of altered blood flow (Fig. 7A). E7386 reduced Axin2 expression in SMA^+ cells in atherosclerotic arteries (fig. S16, A and B), which is again consistent with inhibition of β-catenin C-terminal signaling in vivo. Treatment with E7386 did not affect mouse body weight or serum levels of total cholesterol (fig. S17, A and B) but reduced atherosclerotic lesion expansion (Fig. 7B). In particular, E7386 reduced atherosclerotic lesion area (Fig. 7D), lesion/media ratio (Fig. 7E), and necrotic core area (Fig. 7G). It preserved the lumen cross-sectional area (Fig. 7F) without affecting medial area (Fig. 7C) or fibrous cap thickness (Fig. 7H). In addition, E7386 decreased S1PR1 expression in SMA^+ cells in atherosclerotic arteries (Fig. 7, I and J). Collectively, these findings suggest that pharmacological inhibition of β-catenin C-terminal signaling decreases S1PR1 expression in SMCs and limits atherosclerosis development in this preclinical model.

DISCUSSION

These studies uncover coordination between Wnt/β-catenin and S1PR1 signaling that is essential for vascular remodeling, demonstrating that expression of the β-catenin C terminus in SMCs is required for neointima formation after vascular injury in both female and male mice. Mechanistically, we provide evidence that β-catenin interacts with the *S1pr1* promoter and activates it through its C-terminal domain, which promotes S1PR1 expression and ultimately leads to enhanced SMC growth and robust neointima formation in response to vascular injury. We also show that pharmacologic inhibition of β-catenin C-terminal signaling decreases S1PR1 expression in SMCs, reduces neointima formation after arterial injury, and limits atherosclerosis development.

A previous study from our group using a tamoxifen-inducible and tissue-specific genetic approach found that loss of SMC β-catenin did not affect the structure of carotid arteries of unchallenged mice for 5 weeks after the first tamoxifen administration (*19*). In the present study, we found that inactivation of total β-catenin or its C terminus in SMCs was well tolerated in unchallenged adult mice over 3 months without obvious repercussions for body weight gain, blood pressure, or arterial structure; thus, these signals are not necessary for maintenance of the unstressed, mature state of the vessel.

When the adult arterial wall is disturbed by injury, however, the C-terminal activity of β-catenin becomes essential for SMC proliferation, survival, and neointima formation. The truncated β-catenin encoded by the ΔC allele retains cell adhesion function and N-terminal activity (*31*), so our findings also indicate that other functions of β-catenin (N-terminal signaling and adhesion) in SMCs are not sufficient to drive this phenotype. These findings are consistent with previous studies in mammals, suggesting that β-catenin's adhesion function and/or the N-terminal activity may be less relevant for certain phenotypes in cardiovascular and cancer biology (*23*, *39*, *40*).

Our study also defines β-catenin C-terminal output as an important activator of S1PR1 expression in SMCs. Compelling evidence has established S1PR1 as an essential mediator of endothelial homeostasis (*36*, *41*–*43*). Endothelial β-catenin and/or canonical Wnt signaling have been implicated in related functions, notably blood–brain barrier formation and maintenance (*44*, *45*). Despite this overlap, relatively little is known about how these pathways interact. Wnt/β-catenin and S1P signaling in endothelial cells may be antagonistic in some settings, e.g., during angiogenesis in the developing zebrafish brain, where β-catenin is required to suppress S1PR1 signaling, Rac activation, and premature barrier formation, possibly via effects on cytosolic protein localization (*46*).

Conversely, S1PR1 functions in SMCs appear aligned with the effects of β-catenin. S1PR1 contributes to SMC phenotypic switching and neointima formation after vascular injury. For instance, studies by Kluk and Hla (*13*) found that adult medial SMCs express

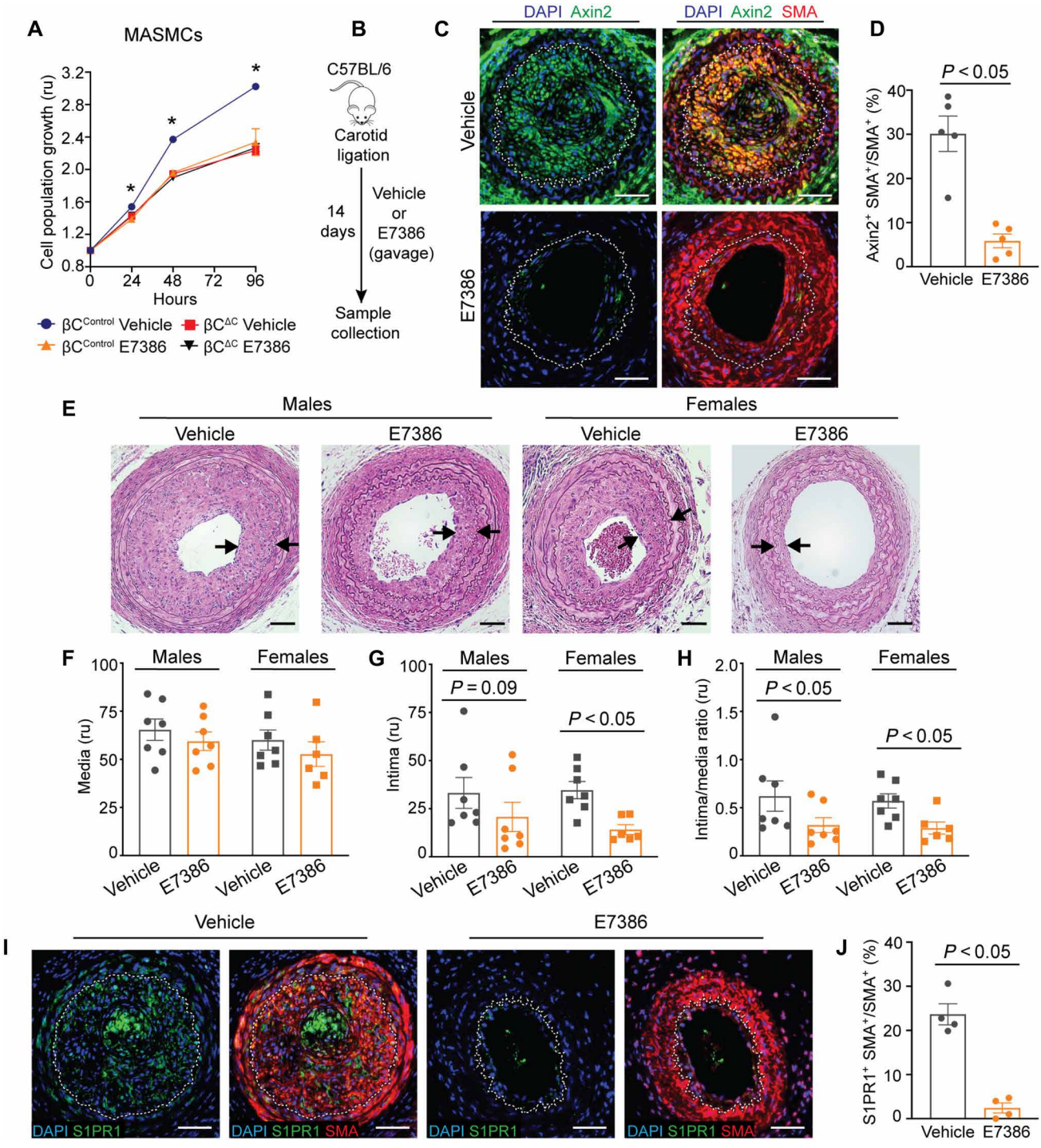

Fig. 6. Pharmacologic inhibition of β-catenin C-terminal signaling attenuates neointimal formation and reduces S1PR1 expression in vivo. (**A**) The β-catenin C-terminal inhibitor E7386 at 100 nM inhibits cell population growth of $\beta C^{Control}$ MASMCs but has no effect on $\beta C^{\Delta C}$ MASMCs. Statistical analysis: Two-way ANOVA with Šídák's multiple comparison test. $n = 6$. *$P < 0.05$ compared to other groups. Data are means ± SEM of independent biological replicates. (**B**) Model schematic—mouse carotid artery ligation was followed by gavage with vehicle or E7386 (50 mg/kg twice daily) before tissue analysis after 14 days. (**C**) E7386 reduces in vivo expression of Axin2, a typical target β-catenin signaling. Right panels show merge of Axin2 and SMA signals (yellow). Dotted line marks the IEL. (**D**) Percentage of SMA^+ cells positive for Axin2. $n = 5$ for each condition. (**E**) Representative images of H&E-stained carotid arteries at 14 days. Arrows delimit the neointimal growth. Scale bars, 50 μm. (**F** to **H**) Morphometric measurements of the medial area (F), intimal area (G), and a ratio of intimal to medial area (H). Each dot represents a single mouse; $n = 7$ for each group except $n = 6$ for E7386-treated females. Statistical analysis: Unpaired Student's *t* test. Values are represented as means ± SEM of independent biological replicates. (**I**) E7386 reduces in vivo expression of S1PR1. Right panels show merge of S1PR1 and SMA signals (yellow). Dotted line marks the IEL. (**J**) Percentage of SMA^+ cells positive for S1PR1. $n = 4$ for each condition. Scale bar, 50 μm. Statistical analysis: Unpaired Student's *t* test. Values are represented as means ± SEM of independent biological replicates.

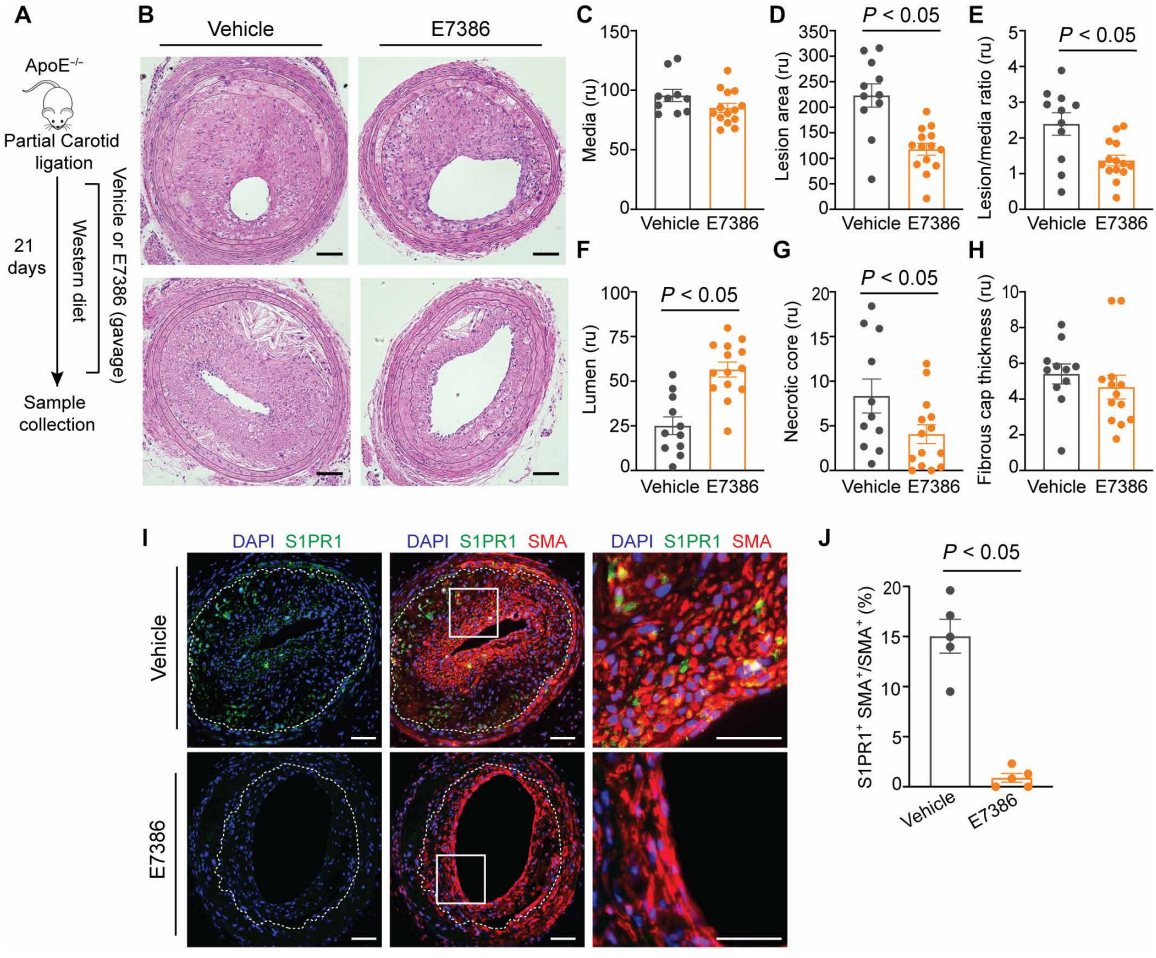

Fig. 7. Pharmacologic inhibition of β-catenin C-terminal signaling limits atherosclerosis and decreases S1PR1 expression in SMCs from atherosclerotic lesions. (**A**) Model schematic—Disturbed flow–induced atherosclerosis in the common carotid artery was induced in male *ApoE*$^{-/-}$ mice by partial carotid artery ligation and Western-type diet feeding, followed by gavage with vehicle or E7386 (25 mg/kg twice daily) before tissue analysis after 21 days. (**B**) Representative images of H&E-stained carotid arteries are shown. Scale bars, 50 μm. (**C** to **H**) Morphometric measurements of the medial area (C), lesion area (D), ratio of lesion to medial area (E), lumen area (F), necrotic core area (G), and fibrous cap thickness (H). Each dot represents a single mouse; $n = 11$ (vehicle) and $n = 14$ (E7386). Statistical analysis: Unpaired Student's *t* test. Values are represented as means ± SEM of independent biological replicates. (**I**) S1PR1 expression. The middle panels show a merge of S1PR1 and SMA signals (yellow), and the white box indicates the inset shown in the right panels. Dotted line marks the IEL. Scale bar, 50 μm. (**J**) Percentage of SMA$^+$ cells positive for S1PR1 in atherosclerotic lesions. Each dot represents a single mouse; $n = 5$ for each condition. Statistical analysis: Unpaired Student's *t* test. Values are represented as means ± SEM of independent biological replicates.

lower *S1pr1* mRNA levels compared to pup-intimal SMCs but have robust proliferative and migratory responses to S1P when submitted to stable transfection or adenoviral delivery of S1PR1, suggesting that up-regulated S1PR1 expression and signaling may be relevant for vascular pathophysiology. Further studies have found that pharmacological inhibition of S1PR1 reduces proliferation and migration of cultured vascular SMCs (*14*, *47*). Moreover, overexpression of S1PR1 or its pharmacological activation attenuated the promoter activity of the *Acta2* gene (which encodes SMA), suggesting that S1PR1 contributes to the suppression of SMC differentiation marker genes, a hallmark of vascular remodeling (*14*). In vivo, S1PR1 expression was found to be increased in the neointima of different animal models of vascular injury (*14*–*17*) and in the neointima of human lesions identified with instent restenosis (*18*). In addition, treatment with VPC44116, an S1PR1 antagonist, attenuated neointima formation after acute balloon injury of the rat carotid artery (*14*).

Despite these observations, the upstream regulation of S1PR1 expression and in vivo relevance of identified mechanisms are not well understood. STAT3 and Kruppel-like factor 2 (KLF2) activate the transcription of *S1pr1* in tumor and T cells, respectively (*48*, *49*), but direct consequences of these mechanisms for in vivo phenotypes remain to be evaluated. STAT3 is also required for leptin-induced S1PR1 protein expression in neurons (*50*), but whether this reflects a direct effect of STAT3 on *S1pr1* transcription was not determined. Understanding of how S1PR1 expression is regulated in vascular systems is also limited. Long intergenic noncoding RNA antisense to S1PR1 (LISPR1) and KLF2 seem to be important for *S1pr1* transcription in cultured endothelial cells (*35*, *51*), but whether these findings extend to the in vivo setting is unknown. Another study found that loss of DJ-1 increased S1PR1 expression in vascular SMCs and in mouse carotid arteries after injury, and also modified the abundance of histone deacetylase 1 and acetylated histone H3 associated with the *S1pr1* promoter of vascular SMCs, suggesting that DJ-1 may contribute to

the epigenetic control of S1PR1 in those cells (*47*). However, if these modifications induced by DJ-1 affect *S1pr1* promoter activity and have a direct, functional implication in vivo is unknown.

In the present study, we demonstrate that β-catenin/TCF4 binds to the *S1pr1* promoter and induces S1PR1 expression through β-catenin C terminus–mediated transcriptional activation. We show that pharmacological activation of WT β-catenin increases S1PR1 expression in SMCs, whereas the same treatment applied to C terminus–deficient β-catenin fails to do so. Moreover, the low levels of S1PR1 observed in β-catenin C terminus–deficient SMCs are restored toward control levels by expression of a full-length β-catenin. In addition, we find that loss of β-catenin C-terminal output decreases *S1pr1* promoter activity and mRNA levels and that the promoter activity is rescued by expression of a constitutively active form of full-length β-catenin, indicating that the C-terminal signaling of β-catenin is necessary for *S1pr1* transcription. Many coactivators are known to bind to the C-terminal domain of β-catenin and thereby to mediate its transcriptional activity (*52*). Our observations suggest that a modified β-catenin that cannot recruit C-terminal coactivators can no longer activate the *S1pr1* promoter, induce S1PR1 protein expression, and thereby stimulate SMC growth and injury-induced neointima formation, identifying a previously unrecognized mechanism by which β-catenin affects SMC biology.

We provide evidence of the functional importance of S1PR1 as a downstream effector of the β-catenin C-terminal signaling. Restoring S1PR1 expression in β-catenin C terminus–deficient SMCs increased cell proliferation toward control levels, while knockdown of S1PR1 in WT MASMCs prevented the increased SMC proliferation induced by β-catenin up-regulation. Notably, restoring S1PR1 expression in SMCs in vivo reestablished neointima formation in mice lacking the β-catenin C-terminal domain in SMCs. Increasing the expression of S1PR1 in SMCs in mice that express full-length β-catenin does not enhance neointima formation after injury, which suggests that the genetic strategy used to increase S1PR1 expression is not sufficient to enhance SMC growth beyond that effected by WT β-catenin via native S1PR1 expression. These in vivo observations support S1PR1 as an effector of β-catenin C-terminal signaling in arterial occlusion after injury. Future studies using an in vivo SMC-specific S1PR1 loss-of-function approach are required to complement what we have learned about the role of S1PR1 in neointima formation after vascular injury.

Our genetic studies provided a rationale for testing whether inhibitors of β-catenin C-terminal signaling limit SMC proliferation and vascular remodeling associated with intimal expansion such as that observed after arterial injury or atherosclerosis. Small molecules specifically designed to inhibit the C-terminal signaling of β-catenin have been developed and are currently being investigated in phase 1 or 2 clinical trials for patients with cancer (*29*, *30*). E7386 is a β-catenin C-terminal inhibitor that can be orally administered and has shown beneficial effects for different tumors (*29*, *53*, *54*); however, it has not been tested in vascular biology or disease. We therefore assessed how E7386 affects neointima formation and atherosclerosis development.

E7386 has been reported to inhibit canonical Wnt signaling–dependent gene expression by preventing the interaction between the β-catenin C terminus and CBP (*29*). A recent study argues that the E7386 mechanism of action does not necessarily involve CBP (*55*). Our studies show that at the concentrations used, E7386 inhibits cell growth of WT SMCs but does not affect growth of β-catenin C terminus–deficient SMCs. This observation does not distinguish among the various possible C-terminal co-activators but supports the idea that E7386 activity in SMCs depends on the β-catenin C terminus. Moreover, our findings show that pharmacologic inhibition of β-catenin C-terminal signaling with E7386 decreases SMC proliferation, attenuates neointima formation after injury, and limits atherosclerosis development. Previous studies have shown that ICG-001, another β-catenin C-terminal inhibitor, reduces pulmonary vascular remodeling in animal models of hyperoxia- or hypoxia-driven pulmonary diseases (*56*–*58*). Our studies provide evidence that pharmacologic inhibition of β-catenin C-terminal signaling has salutary effects in models of common diseases of the systemic vasculature. We found that E7386 decreases S1PR1 expression in SMCs in vitro and in vivo, further supporting the idea that β-catenin C-terminal output controls S1PR1 expression. Collectively these results suggest that inhibitors of the β-catenin C terminus, at least in part by hindering the β-catenin C-terminal/S1PR1 axis, have therapeutic potential for vascular pathologies associated with SMC proliferation and intimal expansion, such as restenosis and atherosclerosis.

While the translational implications of these findings are promising, some limitations of the work merit consideration. For one, our genetic studies used a model of vascular injury, carotid artery ligation, which differs substantially from clinical catheter-based procedures; however, the key attributes of this model—simplicity and reproducibility—facilitated the use of complex genetic strategies in this study. In addition, we have not fully evaluated possible interactions of β-catenin signaling with other S1P receptors, which have complex and non-redundant signaling activities. Similarly, we cannot not rule out that other mechanisms contribute to this phenotype. For example, we previously found that loss of the β-catenin C terminus allows p53 activation in SMCs during vascular development (*23*), but we found no evidence of p53 activation in adult arteries at 21 days after injury (fig. S18)—it remains possible that this mechanism is operative at earlier time points. Last, while our genetic interventions are SMC specific, pharmacological intervention in vivo may act on cell types other than SMCs and have off-target effects.

In summary, we provide evidence that SMC β-catenin C-terminal signaling promotes vascular remodeling by activating the *S1pr1* promoter and inducing S1PR1 expression in vascular SMCs, thereby enhancing vascular SMC proliferation and neointima formation after arterial injury. We also show the translational potential of these findings by evaluating the effects of E7386, a β-catenin C-terminal inhibitor. We provide evidence that E7386 decreases S1PR1 expression in vivo, reduces neointima formation after arterial injury, and attenuates atherosclerosis development in animal models. In addition to identifying β-catenin C-terminal output as a key upstream regulator of S1PR1 expression, these findings open up lines of investigation to develop and apply therapeutic strategies to ameliorate obstructive vascular disease.

MATERIALS AND METHODS

Mice

Ctnnb1$^{\Delta C/flox}$, *Acta2-CreER*^{T2}, and *Rosa26*$^{LSL\text{-}S1pr1}$ mice were generated and validated in previous studies (*23*, *31*, *32*, *36*). *Ctnnb1*$^{flox/flox}$ (B6.129-*Ctnnb1*tm2Kem/KnwJ) and *Rosa26*$^{LSL\text{-}TdTomato/LSL\text{-}TdTomato}$ [*Gt(ROSA)26Sor*$^{tm9(CAG\text{-}tdTomato)Hze}$; also referred to as RFP] mice were obtained from the Jackson Laboratory. *Ctnnb1*$^{WT/WT}$ mice were crossed with *Ctnnb1*$^{flox/flox}$ to generate *Ctnnb1*$^{WT/flox}$ mice. Next, *Ctnnb1*$^{WT/flox}$

mice were crossed with *Acta2-CreER*^{T2} and *Rosa26*$^{LSL\text{-}TdTomato/LSL\text{-}TdTomato}$ mice to generate *Ctnnb1*$^{WT/flox}$;*Rosa26*$^{LSL\text{-}TdTomato/WT}$;*Acta2-CreER*^{T2} mice. Last, *Ctnnb1*$^{\Delta C/flox}$ mice were crossed with *Ctnnb1*$^{WT/flox}$;*Rosa26*$^{LSL\text{-}TdTomato/WT}$;*Acta2-CreER*^{T2} mice to generate *Ctnnb1*$^{\Delta C/flox}$;*Rosa26*$^{LSL\text{-}TdTomato/WT}$;*Acta2-CreER*^{T2} mice and their littermate controls *Ctnnb1*$^{WT/flox}$;*Rosa26*$^{LSL\text{-}TdTomato/WT}$;*Acta2-CreER*^{T2}. These mice were treated with tamoxifen to remove the β-catenin flox allele, resulting in mice bearing the ΔC allele (referred to as SMβC$^{\Delta C}$ mice) or the WT allele (referred to as SMβC$^{WT/-}$ mice) as the only sources of β-catenin in SMCs. In addition, tamoxifen administration also activates RFP for SMC lineage tracing. For tamoxifen-inducible, SMC-specific gain of function of *S1pr1* gene, *Ctnnb1*$^{WT/flox}$;*Rosa26*$^{LSL\text{-}TdTomato/WT}$;*Acta2-CreER*^{T2} mice were initially crossed with *Rosa26*$^{LSL\text{-}S1pr1}$ mice to generate *Ctnnb1*$^{WT/flox}$;*Rosa26*$^{LSL\text{-}TdTomato/LSL\text{-}S1pr1}$;*Acta2-CreER*^{T2} mice. Next, *Ctnnb1*$^{\Delta C/flox}$;*Rosa26*$^{LSL\text{-}TdTomato/WT}$ mice were crossed with *Ctnnb1*$^{WT/flox}$;*Rosa26*$^{LSL\text{-}TdTomato/LSL\text{-}S1pr1}$;*Acta2-CreER*^{T2} mice that yielded *Ctnnb1*$^{\Delta C/flox}$;*Rosa26*$^{LSL\text{-}TdTomato/LSL\text{-}S1pr1}$;*Acta2-CreER*^{T2} mice (referred to as SMβC$^{\Delta C}$ SM-S1PR1^{GOF} mice after tamoxifen administration) and their littermate controls *Ctnnb1*$^{WT/flox}$;*Rosa26*$^{LSL\text{-}TdTomato/LSL\text{-}S1pr1}$;*Acta2-CreER*^{T2} (referred to as SMβC$^{WT/-}$ SM-S1PR1^{GOF} mice after tamoxifen administration). Male and female 8- to 16-week-old mice were used as breeders for timed mating. Methods for mouse tail genotyping by PCR for *Ctnnb1*$^{\Delta C/flox}$, *Rosa26*$^{LSL\text{-}S1pr1}$, *Ctnnb1*$^{flox/flox}$, and *Acta2-CreER*^{T2} mice have been previously described (*23*, *31*, *32*, *36*, *59*), and genotyping for *Rosa26*$^{LSL\text{-}TdTomato}$ mice was performed according to a Jackson Laboratory protocol. WT C57BL/6J (strain #000664) and *ApoE*$^{-/-}$ (strain #002052) mice used in the pharmacologic studies were purchased from the Jackson Laboratory. All animals were housed in pathogen-free conditions; the procedures followed the rules and regulations of the Association for Assessment and Accreditation of Laboratory Animal Care and were approved by the Institutional Animal Care and Use Committee of Albert Einstein College of Medicine.

Tamoxifen administration

Under pathogen-free conditions, 100 mg of tamoxifen (STEMCELL Technologies, no. 72662) was dissolved in 0.5 ml of ethanol (Decon Laboratories Inc., 22032601), and 9.5 ml of corn oil (Sigma-Aldrich, C8267) was added to achieve a final concentration of 10 mg/ml. Eight- to 9-week-old male and female mice were given 100 μl (1 mg) of tamoxifen solution via intraperitoneal injection daily for five consecutive days. Carotid artery ligation was performed 1 week after the first injection.

Carotid artery ligation

Carotid artery ligation has already been described (*19*). Briefly, 9- to 10-week-old male and female mice were anesthetized with ketamine/xylazine (90 and 10 mg/kg, respectively) via intraperitoneal injection. A 5-mm skin incision on the base of the neck and blunt dissection were performed until the left common carotid artery was exposed. The artery was separated from surrounding tissues and ligated with 6-0 silk (Ethicon, K889H) just proximal to the bifurcation. The right common carotid artery served as control. The incision was closed, and mice were allowed to recover. Meloxicam (5 mg/kg) was administered subcutaneously after carotid ligation for pain relief. Carotid arteries were harvested 21 days after ligation. Mice were euthanized by ketamine/xylazine injection plus thoracotomy, and the systemic circulation was flushed with phosphate-buffered solution (PBS) and then perfused with 10% formalin phosphate buffer (Fisher Scientific, SF100-4) for 7 min. Left and right carotid arteries were removed and postfixed in 10% formalin phosphate buffer overnight, followed by 70% ethanol. Tissues required for DNA, RNA, or protein isolation were harvested, snap-frozen, and kept at −80°C until processing.

E7386 treatment after carotid artery ligation

For in vivo administration, E7386 (Chemietek, CT-E7386) was dissolved in 0.01 M HCl. After carotid artery ligation, 9- to 10-week-old male and female WT C57BL/6J mice were given E7386 (50 mg/kg) or vehicle (0.01 M HCl) by oral gavage twice daily for 14 days. Carotid arteries were harvested 14 days after ligation, following the same procedures described above.

Processing and morphometric analysis of injured carotid arteries

Fixed carotid arteries were trimmed under a Stemi 2000-C stereomicroscope (Zeiss) such that 3 mm of vessel adjacent to the ligation point was left available for analysis. Trimmed arteries were processed and paraffin-embedded with the ligature on top. Paraffin blocks were trimmed until a full cross section of the ligated artery was visualized; thereafter, in sequence, the next 400 μm of tissue was discarded, 180 μm was collected for analysis (5-μm-thick sections, three sections per slide, 12 slides), 400 μm was discarded, 180 μm was collected for analysis, 400 μm was discarded, and 180 μm was collected for analysis. This protocol allowed the evaluation of vascular remodeling at three consistent distances from the ligation site in each artery. Arterial cross sections were stained with hematoxylin and eosin (H&E) and photographed with a Leica DMi8 inverted microscope. Morphometric analysis of carotid arteries was performed using ImageJ software as follows: the area of the lumen, the area inside the internal elastic lamina (IEL), and the area inside the external elastic lamina (EEL) were measured in pixels. The area of the intima was calculated by subtracting the area of the lumen from the area inside the IEL. The area of the media was calculated by subtracting the area inside the IEL from the area inside the EEL. Last, the intima/media ratio was calculated.

Atherosclerosis studies

Disturbed flow–induced atherosclerosis in the common carotid artery was induced in 8- to 10-week-old male *ApoE*$^{-/-}$ mice by partial carotid artery ligation and Western-type diet feeding, following procedures previously described (*38*). Briefly, mice were anesthetized with ketamine/xylazine (90 and 10 mg/kg, respectively) via intraperitoneal injection. A 5-mm skin incision on the base of the neck and blunt dissection were performed until the left common carotid artery was exposed. Three of four caudal branches of the left common carotid artery (left external carotid, internal carotid, and occipital artery) were ligated with 6-0 silk (Ethicon K889H), while the superior thyroid artery was left intact. The incision was closed, and mice were allowed to recover. Meloxicam (5 mg/kg) was administered subcutaneously after carotid ligation for pain relief. After surgery, mice were placed for 21 days on Western diet (Envigo TD.88137; 42% kcal from fat, 0.2% total cholesterol, saturated fat >60% total fat, and high sucrose) and orally administered with E7386 (25 mg/kg) or vehicle (0.01 M HCl) by oral gavage twice daily for 21 days. Blood and carotid arteries were harvested 21 days after ligation. Mice were euthanized by ketamine/xylazine injection plus thoracotomy, and the systemic circulation was flushed with PBS and then perfused with 10% formalin phosphate buffer (Fisher Scientific, SF100-4) for

7 min. Left and right carotid arteries were removed and postfixed in 10% formalin phosphate buffer overnight, followed by 70% ethanol. Blood samples were obtained by cardiac puncture before PBS perfusion, and serum was obtained by centrifugation at 6000*g* for 10 min at 4°C, snap-frozen, and stored at −80°C until further use. Serum levels of total cholesterol were measured using the Cholesterol Quantification Assay kit (Sigma-Aldrich, CS0005-1KT).

Processing and morphometric analysis of atherosclerotic lesions

Fixed carotid arteries were processed and paraffin-embedded with the ligature on top. Paraffin blocks were trimmed until a full cross section of the ligated artery was visualized; thereafter, in sequence, the next 240 μm of tissue was collected for analysis (5-μm-thick sections, four sections per slide, 12 slides), 500 μm was discarded, 240 μm was collected for analysis, 500 μm was discarded, 240 μm was collected for analysis, 500 μm was discarded, 240 μm was collected for analysis, 500 μm was discarded, and 240 μm was collected for analysis. This protocol allowed the evaluation of atherosclerotic lesions at five consistent distances from the ligation site in each artery. Arterial cross sections were stained with H&E and photographed with a Leica DMi8 inverted microscope. Morphometric analysis of carotid arteries was performed using ImageJ software as follows: The area of the lumen, the area inside the IEL, and the area inside the EEL were measured in pixels. The lesion area was calculated by subtracting the area of the lumen from the area inside the IEL. The area of the media was calculated by subtracting the area inside the IEL from the area inside the EEL, and the lesion/media ratio was calculated. Necrotic cores were quantified as previously described (*60*), defined as the H&E-negative acellular areas in the intima. The fibrous cap thickness was quantified by choosing the largest necrotic core in a section and measuring the thinnest part of the cap, from its outer edge to the necrotic core boundary.

Vascular homeostasis studies

Baseline blood pressure and body weight of 8- to 9-week-old male and female mice were recorded just before the first tamoxifen administration and followed for 12 weeks after the last tamoxifen injection, at 2-week intervals. Blood pressure was measured as described in the next section. Thoracic aortas and carotid arteries were harvested 12 weeks after the last tamoxifen injection. Mice were euthanized by ketamine/xylazine injection plus thoracotomy, and the vascular system was flushed with PBS and then perfused with 10% formalin phosphate buffer (Fisher Scientific, SF100-4) for 7 min. Aortas and carotid arteries were removed and postfixed in 10% formalin phosphate buffer overnight, followed by 70% ethanol, and then embedded in paraffin. The serial cuts at 5-μm-thick sections were done using the paraffin blocks. The cuts were stained with H&E and photographed with a Leica DMi8 inverted microscope. Morphometric analysis of medial area of aortas and carotid arteries was performed using ImageJ software. The area inside the IEL and the area inside the EEL were measured in pixels. The area of the media was calculated by subtracting the area inside the IEL from the area inside the EEL.

Blood pressure measurements

Systolic blood pressure was measured in conscious male and female mice using the tail-cuff method (Kent Scientific Inc.). Briefly, animals were placed in a mouse restrainer (RTBP007, Kent Scientific Inc.), and a mouse occlusion cuff (RTBP050, Kent Scientific Inc.) and mouse plethysmographic cuff (XBP051, Kent Scientific Inc.) were applied to the tail of the mouse. Mice were trained for 1 week to become accustomed to the new handling and environment. Systolic blood pressure measurements were taken using the XBP1000 apparatus (Kent Scientific Inc.) connected to a data acquisition system. Five consecutive measurements were performed per mouse, per time point, and the values were averaged. Measurements were done at the same time of the day at the indicated time points.

Immunofluorescence of arteries

Tissue sections were deparaffinized and rehydrated, and antigen retrieval was performed by boiling in sodium citrate solution (Vector Labs, H-3300). Tissues were blocked in 0.3% Triton X-100, 2% bovine serum albumin, and 5% normal horse serum in PBS for 1 hour at room temperature. Tissues were incubated overnight at 4°C in blocking solution with the following primary antibodies: anti–β-catenin targeting the C terminus (1:50 dilution; Santa Cruz Biotechnology, sc-7963); anti–β-catenin targeting the N terminus (1:100 dilution; Cell Signaling Technology, 9562S); anti-RFP anti-rabbit (1:200 dilution; Rockland, 600-401-379), anti-RFP anti-mouse (1:100 dilution; Invitrogen, MA5-15257), anti-Axin2 (1:100 dilution; Invitrogen, PA5-21093), anti-CD31 (1:50 dilution; Abcam, 28364), anti-SMA (1:200 dilution; Santa Cruz Biotechnology, sc-32251), anti-Ki67 (1:50 dilution; Abcam, 15580), anti-PCNA (1:100 dilution; Invitrogen, 13-3900), anti–cleaved caspase-3 (1:50 dilution; Cell Signaling Technology, 9661), and anti-S1PR1 (1:100 dilution; Invitrogen, PA1-1040). After washing, sections were incubated for 1 hour at room temperature with fluorochrome-conjugated secondary antibodies Alexa Fluor 488 goat anti-mouse (1:200 dilution; Invitrogen, A32723) and Alexa Fluor 546 donkey anti-rabbit (1:400 dilution; Invitrogen, A10040) in blocking solution. After washing, sections were stained with 4′,6-diamidino-2-phenylindole (DAPI) during mounting (FLUORO-GEL II, with DAPI, Electron Microscopy Sciences, 17985-50). Fluorescence emission was visualized with a Leica DMi8 inverted microscope. Subsequent image processing and quantification of fluorescent signal were achieved by using the National Institutes of Health (NIH) Fiji program. For Ki67 and PCNA staining, only the nuclear signals were included in the quantification. Specificity of staining was confirmed by omission of the primary antibody.

Mouse aortic SMCs

Primary MASMCs were isolated from 5- to 6-week-old male and female *Ctnnb1*$^{\Delta C/flox}$ and *Ctnnb1*$^{\Delta C/flox}$*;Rosa26*$^{LSL\text{-}S1pr1/LSL\text{-}TdTomato}$ mice using collagenase-elastase digestion as described before (*19*), maintained in Dulbecco's modified Eagle medium plus 20% fetal bovine serum, penicillin (100 U/ml), streptomycin (100 μg/ml), and 2 mM L-glutamine, and subcultured weekly. Passage 2 of cells isolated from *Ctnnb1*$^{\Delta C/flox}$ mice was transduced with adenovirus expressing GFP (Ad5.CMV-GFP) or Cre (Ad5.CMV-Cre) to generate control (βC^{Control}) or β-catenin C terminus–deficient (βC$^{\Delta C}$) cells, respectively. Passage 2 of cells isolated from *Ctnnb1*$^{\Delta C/flox}$*;Rosa26*$^{LSL\text{-}S1pr1/LSL\text{-}TdTomato}$ mice was transduced with adenovirus expressing GFP (Ad5.CMV-GFP) or Cre (Ad5.CMV-Cre) to generate control (βC^{Control} S1PR1^{Control}) or βC$^{\Delta C}$ cells with S1PR1 GOF (βC$^{\Delta C}$ S1PR1^{GOF}), respectively. Passages 3 to 6 were used for experiments. To evaluate how the inhibition of β-catenin degradation affects S1PR1 expression, we treated βC^{Control} and βC$^{\Delta C}$ MASMCs with CHIR99021 (Cell Signaling Technology, 54290S) for 48 hours. CHIR99021 was dissolved in dimethyl

sulfoxide (DMSO) to obtain a stock solution at 10 mM. Dilutions from the stock solution in culture medium were performed to test final concentrations from 0.1 to 1 μM. Same dilution protocols were used with only DMSO to generate vehicle controls specific for each concentration. To evaluate the effects of the pharmacologic inhibition of β-catenin C terminus, we treated $\beta C^{Control}$ and $\beta C^{\Delta C}$ MASMCs with E7386 (Chemietek, CT-E7386), which was dissolved in DMSO to obtain a stock solution at 10 mM. Dilutions from the stock solution in culture medium were performed to test final concentrations from 10 to 100 nM. Same dilution protocols were used with only DMSO to generate vehicle controls specific for each concentration.

Cell population growth

To evaluate the effect of genetic interventions on growth of MASMCs, 4×10^3 cells per well were plated in 96-well plates with a minimum of four independent wells per group. Evaluation of cell growth in culture was performed with the AlamarBlue assay (BUF012A, Bio-Rad), and absorbances at 570 and 600 nm were measured on a Varioskan LUX multimode microplate reader (Thermo Fisher Scientific). AlamarBlue reduction correlates with the number of viable cells and was calculated according to the manufacturer's instructions and expressed as fold change with respect to baseline.

Cell transfection

$\beta C^{Control}$ and $\beta C^{\Delta C}$ MASMCs were transfected with pcDNA3-β-catenin^{S33Y} (constitutively active β-catenin) or empty vector using the electroporation method. The electroporation was performed using a Neon transfection system (Invitrogen). Electroporated cells were plated in antibiotic-free medium in a 24-well plate for 24 hours and then switched to regular medium. Triplicates for every group and condition were used every time. Cell lysates were collected 72 hours after electroporation for Western blotting experiments.

Small interfering RNA

The siRNA targeting mouse *S1pr1* was synthesized by Thermo Fisher Scientific (Silencer Select, 4390771, assay ID s65292). Transient transfection of siRNA (10 nM) was performed by using Lipofectamine RNAiMAX (Thermo Fisher Scientific, 13778150), as recommended by the manufacturer. Control cells were transfected with 10 nM Silencer Select negative control siRNA (Thermo Fisher Scientific, 4390843). After 24 hours, cells were treated with CHIR99021 (Cell Signaling Technology, 54290S) or vehicle, and the cell population growth was evaluated 48 and 72 hours after plating.

Western blotting

Protein lysates were extracted from SMCs or blood vessels using radioimmunoprecipitation assay buffer [50 mM tris-HCl (pH 7.4), 1% NP-40, 0.5% sodium deoxycholate, 0.1% SDS, 1 mM EDTA, and 150 mM NaCl] plus protease inhibitors (Complete Mini Roche Life Science, 04693159001). A BCA protein assay kit (Pierce, 23335) was used to measure protein concentrations, and equal amounts of protein were loaded (20 to 60 μg) and separated by 10% polyacrylamide gel electrophoresis. Proteins were transferred (Trans-Blot SD cell, Bio-Rad, 170-3940) to 0.45-μm pore size polyvinylidene difluoride membranes (Immobilon-P, Millipore), blocked for 1 hour at room temperature with TBST [tris (pH 8.0), NaCl 150 mM, and 0.1% Tween 20] plus 5% (w/v) nonfat milk or 6% bovine serum, and incubated overnight at 4°C in blocking solution with the following primary antibodies: anti–β-catenin targeting the C terminus (1:500 dilution; Santa Cruz Biotechnology, sc-7963), anti–β-catenin targeting the N terminus (1:250 dilution; Cell Signaling Technology, 9562S), anti-S1PR1 (1:1000 dilution; Millipore, MABC94), anti-S1PR3 (1:1000 dilution; Alomone, ASR-013), anti-Axin2 (1:1000 dilution; Invitrogen, PA5-21093), and anti–glyceraldehyde-3-phosphate dehydrogenase (GAPDH) (1:5000 dilution; Santa Cruz Biotechnology, sc-25778). After washing, membranes were incubated with horseradish peroxidase–conjugated secondary antibodies for 1 hour at room temperature. After washing, signals were detected by adding enhanced chemiluminescence (ECL) substrate (ECL Western Blotting Substrate, Pierce 32106) and exposing films to membranes. Densitometric analysis was performed with ImageJ.

Standard RNA-seq library preparation with rRNA depletion and HiSeq sequencing

Total RNA was isolated from $\beta C^{Control}$ and $\beta C^{\Delta C}$ MASMCs using TRIzol reagent (Invitrogen, 15596018) according to the manufacturer's instructions. RNA concentrations were calculated using NanoDrop technology (Thermo Fisher Scientific, ND-1000), and RNA integrity was evaluated using RNA 6000 Nano LabChips on an Agilent 2100 Bioanalyzer (Agilent Technologies). Sample quality control, library preparations, and sequencing reactions for RNA-seq were conducted at GENEWIZ LLC. (South Plainfield, NJ, USA). Ribosomal RNA (rRNA) depletion was performed using Ribo-Zero Gold Kit (Human/Mouse/Rat probe) (Illumina, San Diego, CA, USA). RNA-seq library preparation used NEBNext Ultra II RNA Library Preparation Kit for Illumina by following the manufacturer's recommendations (New England Biolabs, Ipswich, MA, USA). Briefly, enriched RNAs were fragmented for 15 min at 94°C. First-strand and second-strand cDNAs were subsequently synthesized. Following procedures previously described (*61*), cDNA fragments were end-repaired and adenylated at 3′ ends, and universal adapters were ligated to cDNA fragments, followed by index addition and library enrichment with limited cycle PCR. Sequencing libraries were validated using the Agilent Tapestation 4200 (Agilent Technologies, Palo Alto, CA, USA) and quantified using Qubit 4.0 Fluorometer (Invitrogen, Carlsbad, CA) as well as by quantitative PCR (Applied Biosystems, Carlsbad, CA, USA). The sequencing libraries were multiplexed and clustered onto a flow cell and loaded on the Illumina HiSeq4000 or equivalent instrument according to the manufacturer's instructions. The libraries were sequenced using a 2 × 150 paired-end configuration. Raw sequence data (.bcl files) generated from Illumina instrument were converted into FASTQ files and de-multiplexed using Illumina's bcl-2fastq 2.17 software. One mismatch was allowed for index sequence identification.

Standard RNA-seq data analysis

After investigating the quality of the raw data, sequence reads were trimmed to remove possible adapter sequences and nucleotides with poor quality using Trimmomatic v.0.36. The trimmed reads were mapped to the *Mus musculus* reference genome available on ENSEMBL using the STAR aligner v.2.5.2b. The STAR aligner uses a splice aligner that detects splice junctions and incorporates them to help align the entire read sequences. BAM files were generated as a result of this step. Unique gene hit counts were calculated by using featureCounts from the Subread package v.1.5.2. Only unique reads that fell within exon regions were counted. Because a strand-specific library preparation was performed, the reads were strand-specifically counted. After extraction of gene hit counts, the gene hit counts

table was used for downstream differential expression analysis. Using DESeq2, a comparison of gene expression between the groups of samples was performed. The Wald test was used to generate *P* values and $\log_2$ fold changes. Genes with adjusted *P* values <0.05 and absolute $\log_2$ fold changes >1 were called as differentially expressed genes for each comparison. A PCA analysis was performed using the "plotPCA" function within the DESeq2 R package. The plot shows the samples in a two-dimensional plane spanned by their first two principal components. The top 500 genes, selected by highest row variance, were used to generate the plot (*61*). Pathway analysis was performed using the IPA system (version 76765844, Qiagen) including the differentially expressed genes, with threshold defined as −log (*P* value) of >1.3.

Real-time qPCR

Total RNA isolated from $\beta C^{Control}$ and $\beta C^{\Delta C}$ MASMCs was reverse-transcribed to cDNA using SuperScript III first-strand synthesis system (Invitrogen, 18080-051). cDNA was quantified using an SYBR Green qPCR kit (Applied Biosystems, catalog no. 4309155) and ViiA7 Real-time PCR system (Applied Biosystems). The data were analyzed with $2^{-\Delta Ct}$ method in which ΔCt was calculated between the gene of interest and housekeeping gene, *Rpl13* and β-*actin*. The following primer sequences were used: *Axin2*, 5′-gagagtgagcggcagagc-3′ (forward) and 5′-cggctgactcgttctcct-3′ (reverse); β-*actin*, 5′-ctaaggccaaccgtgaaaag-3′ (forward) and 5′-accagaggcatacagggaca-3′ (reverse); *Rpl13*, 5′-gcttacctggggcgtctg-3′ (forward) and 5′-acattcttttctgcctgtttcc-3′ (reverse); *S1pr1*, 5′-cggtgtagacccagagtcct-3′ (forward) and 5′-agcttttccttggctggag-3′ (reverse); and *S1pr3*, 5′-agatgcgccttgcagaac-3′ (forward) and 5′-gtggtggtgggttcctga-3′ (reverse).

Luciferase assay

$\beta C^{Control}$ and $\beta C^{\Delta C}$ MASMCs (5×10^4 per well) were electroporated with pCMV-β-gal (transfection control) and with pGL3-*S1pr1*-promoter (provided by J. Garcia, University of Arizona) (*35*). When indicated, pcDNA3-β-$catenin^{S33Y}$ or empty vector was also included in the electroporation protocol. Electroporation was performed as described above. Cell lysates were collected 72 hours after electroporation, and luciferase activity was determined using the Glo-lysis buffer system (Promega) and the Varioskan LUX multimode microplate reader (Thermo Fisher Scientific). Luciferase activities were normalized to β-galactosidase activity for each well to control for transfection efficiency.

Cleavage under targets and release using nuclease assay

CUT&RUN was performed using the CUT&RUN Assay Kit (Cell Signaling Technology, 86652). Briefly, 50,000 cells were washed in wash buffer and bound to 10 μl of activated concanavalin A beads. Bead-bound cells were incubated with primary antibodies at 4°C overnight in antibody binding buffer. β-Catenin (Antibodies Online, ABIN2855042), TCF4 (Cell Signaling Technology, 2569S), and rabbit immunoglobulin G (IgG) (Cell Signaling Technology, DA1E) primary antibodies validated for CUT&RUN were used. Then, the cell-bead mixture was washed with wash buffer and incubated with protein A–Micrococcal Nuclease for 1 hour at 4°C. After washing with wash buffer, 2 mM $CaCl_2$ was added to the samples to activate protein A–MNase digestion for 30 min on ice. The reaction was stopped with the addition of 2× stop buffer containing 20 mM EDTA, 0.05% digitonin, and ribonuclease A (5 mg/ml). Released chromatin fragments were purified using phenol/chloroform extraction and ethanol precipitation. The eluted DNA was analyzed by qPCR to determine β-catenin and TCF4 enrichment on the *S1pr1* promoter. The sequences of the primers for the *S1pr1* promoter were 5′-gcttcactctcctcccacaa (forward) and 5′-tctgctcaaatgctgtcaatc (reverse) (fragment −1973/−1802); 5′-tgaactgctgctggattgtt (forward) and 5′-gtgctgtgcttgatgttgga (reverse) (fragment −939/−790); and 5′-ccttctcaggatcccctctc (forward) and 5′-agccctgaggatccgtgtag (reverse) (fragment −638/−512). A primer set that amplifies an 82–base pair fragment in a gene desert on mouse chromosome 6 was used as a negative control (Active Motif, 71011). Anti-H3 antibody and ribosomal protein L30 primers provided by the kit were used as a positive control for the assay technique and reagent integrity.

Statistics

Data were graphed, and statistics were performed using GraphPad Prism version 9.4.1. The data presentation and statistical analyses are described in the figure legends. To determine the number of mice necessary for adequate statistical power, power analysis was performed using preliminary datasets. None of the animals were excluded from the study. Animals were randomly assigned to vehicle or E7386 treatments. Data collection and analyses were conducted blinded to the samples. Blinding was removed only for the final statistical analysis. At least three independent experiments with minimum of three biological replicates were done. Results are presented as mean ± SEM of at least three independent biological replicates in all figures. Before statistical testing, normality was assessed using the Shapiro-Wilk test. For data confirmed to be normally distributed, we used Student's unpaired two-tailed *t* test for comparisons between two groups and one-way analysis of variance (ANOVA) or two-way ANOVA with Tukey's or Šídák's multiple comparisons test for data comparing three or more groups. For data not normally distributed, equivalent nonparametric tests were instead performed, as indicated in the figure legends. Statistically significant differences were defined as $P < 0.05$.

Study approval

This research complies with all relevant ethical regulations. Animal experiments were conducted in accordance with NIH guidelines under protocols 00001011 and 00001583 approved by the Institutional Animal Care and Use Committee of the Albert Einstein College of Medicine.

Supplementary Materials

This PDF file includes:

Figs. S1 to S18

REFERENCES AND NOTES

1. G. A. Roth, G. A. Mensah, C. O. Johnson, G. Addolorato, E. Ammirati, L. M. Baddour, N. C. Barengo, A. Z. Beaton, E. J. Benjamin, C. P. Benziger, A. Bonny, M. Brauer, M. Brodmann, T. J. Cahill, J. Carapetis, A. L. Catapano, S. S. Chugh, L. T. Cooper, J. Coresh, M. Criqui, N. DeCleene, K. A. Eagle, S. Emmons-Bell, V. L. Feigin, J. Fernandez-Sola, G. Fowkes, E. Gakidou, S. M. Grundy, F. J. He, G. Howard, F. Hu, L. Inker, G. Karthikeyan, N. Kassebaum, W. Koroshetz, C. Lavie, D. Lloyd-Jones, H. S. Lu, A. Mirijello, A. M. Temesgen, A. Mokdad, A. E. Moran, P. Muntner, J. Narula, B. Neal, M. Ntsekhe, G. Moraes de Oliveira, C. Otto, M. Owolabi, M. Pratt, S. Rajagopalan, M. Reitsma, A. L. P. Ribeiro, N. Rigotti, A. Rodgers, C. Sable, S. Shakil, K. Sliwa-Hahnle, B. Stark, J. Sundstrom, P. Timpel, I. M. Tleyjeh, M. Valgimigli, T. Vos, P. K. Whelton, M. Yacoub, L. Zuhlke, C. Murray, V. Fuster, GBD-NHLBI-JACC Global Burden of Cardiovascular Diseases Writing Group, Global Burden of Cardiovascular Diseases and Risk Factors, 1990-2019: Update from the GBD 2019 Study. *J. Am. Coll. Cardiol.* **76**, 2982–3021 (2020).

2. M. R. Alexander, G. K. Owens, Epigenetic control of smooth muscle cell differentiation and phenotypic switching in vascular development and disease. *Annu. Rev. Physiol.* **74**, 13–40 (2012).
3. P. Lacolley, V. Regnault, A. Nicoletti, Z. Li, J. B. Michel, The vascular smooth muscle cell in arterial pathology: A cell that can take on multiple roles. *Cardiovasc. Res.* **95**, 194–204 (2012).
4. A. Cartier, T. Hla, Sphingosine 1-phosphate: Lipid signaling in pathology and therapy. *Science* **366**, eaar5551 (2019).
5. V. A. Blaho, T. Hla, An update on the biology of sphingosine 1-phosphate receptors. *J. Lipid Res.* **55**, 1596–1608 (2014).
6. N. Brakch, O. Dormond, S. Bekri, D. Golshayan, M. Correvon, L. Mazzolai, B. Steinmann, F. Barbey, Evidence for a role of sphingosine-1 phosphate in cardiovascular remodelling in Fabry disease. *Eur. Heart J.* **31**, 67–76 (2010).
7. A. J. Fegley, W. J. Tanski, E. Roztocil, M. G. Davies, Sphingosine-1-phosphate stimulates smooth muscle cell migration through galpha(i)- and PI3-kinase-dependent p38(MAPK) activation. *J. Surg. Res.* **113**, 32–41 (2003).
8. K. Lockman, J. S. Hinson, M. D. Medlin, D. Morris, J. M. Taylor, C. P. Mack, Sphingosine 1-phosphate stimulates smooth muscle cell differentiation and proliferation by activating separate serum response factor co-factors. *J. Biol. Chem.* **279**, 42422–42430 (2004).
9. W. Shi, Q. Wang, J. Wang, X. Yan, W. Feng, Q. Zhang, C. Zhai, L. Chai, S. Li, X. Xie, M. Li, Activation of yes-associated protein mediates sphingosine-1-phosphate-induced proliferation and migration of pulmonary artery smooth muscle cells and its potential mechanisms. *J. Cell. Physiol.* **236**, 4694–4708 (2021).
10. K. J. Sattler, S. Elbasan, P. Keul, M. Elter-Schulz, C. Bode, M. H. Graler, M. Brocker-Preuss, T. Budde, R. Erbel, G. Heusch, B. Levkau, Sphingosine 1-phosphate levels in plasma and HDL are altered in coronary artery disease. *Basic Res. Cardiol.* **105**, 821–832 (2010).
11. D. H. Deutschman, J. S. Carstens, R. L. Klepper, W. S. Smith, M. T. Page, T. R. Young, L. A. Gleason, N. Nakajima, R. A. Sabbadini, Predicting obstructive coronary artery disease with serum sphingosine-1-phosphate. *Am. Heart J.* **146**, 62–68 (2003).
12. L. Rotheudt, E. Moritz, M. R. P. Markus, D. Albrecht, H. Volzke, N. Friedrich, E. Schwedhelm, G. Daum, U. Schminke, S. B. Felix, B. H. Rauch, M. Dorr, M. Bahls, Sphingosine-1-phosphate and vascular disease in the general population. *Atherosclerosis* **350**, 73–81 (2022).
13. M. J. Kluk, T. Hla, Role of the sphingosine 1-phosphate receptor EDG-1 in vascular smooth muscle cell proliferation and migration. *Circ. Res.* **89**, 496–502 (2001).
14. B. R. Wamhoff, K. R. Lynch, T. L. Macdonald, G. K. Owens, Sphingosine-1-phosphate receptor subtypes differentially regulate smooth muscle cell phenotype. *Arterioscler. Thromb. Vasc. Biol.* **28**, 1454–1461 (2008).
15. T. Kitano, S. Usui, S. I. Takashima, O. Inoue, C. Goten, A. Nomura, K. Yoshioka, M. Okajima, S. Kaneko, Y. Takuwa, M. Takamura, Sphigosine-1-phosphate receptor 1 promotes neointimal hyperplasia in a mouse model of carotid artery injury. *Biochem. Biophys. Res. Commun.* **511**, 179–184 (2019).
16. J. Braetz, A. Becker, M. Geissen, A. Larena-Avellaneda, S. Schrepfer, G. Daum, Sphingosine-1-phosphate receptor 1 regulates neointimal growth in a humanized model for restenosis. *J. Vasc. Surg.* **68**, 201S–207S (2018).
17. H. Liu, H. Jin, X. Yue, J. Han, P. Baum, D. R. Abendschein, Z. Tu, PET study of sphingosine-1-phosphate receptor 1 expression in response to vascular inflammation in a rat model of carotid injury. *Mol. Imaging* **16**, 153601211668977 (2017).
18. D. Zohlnhofer, T. Richter, F. Neumann, T. Nuhrenberg, R. Wessely, R. Brandl, A. Murr, C. A. Klein, P. A. Baeuerle, Transcriptome analysis reveals a role of interferon-γ in human neointima formation. *Mol. Cell* **7**, 1059–1069 (2001).
19. D. F. Riascos-Bernal, P. Chinnasamy, J. N. Gross, V. Almonte, L. Egana-Gorrono, D. Parikh, S. Jayakumar, L. Guo, N. E. S. Sibinga, Inhibition of smooth muscle β-catenin hinders neointima formation after vascular injury. *Arterioscler. Thromb. Vasc. Biol.* **37**, 879–888 (2017).
20. N. Lyashenko, M. Winter, D. Migliorini, T. Biechele, R. T. Moon, C. Hartmann, Differential requirement for the dual functions of β-catenin in embryonic stem cell self-renewal and germ layer formation. *Nat. Cell Biol.* **13**, 753–761 (2011).
21. T. Valenta, G. Hausmann, K. Basler, The many faces and functions of β-catenin. *EMBO J.* **31**, 2714–2736 (2012).
22. Y. Xing, K. Takemaru, J. Liu, J. D. Berndt, J. J. Zheng, R. T. Moon, W. Xu, Crystal structure of a full-length β-catenin. *Structure* **16**, 478–487 (2008).
23. D. F. Riascos-Bernal, P. Chinnasamy, L. L. Cao, C. M. Dunaway, T. Valenta, K. Basler, N. E. Sibinga, β-Catenin C-terminal signals suppress p53 and are essential for artery formation. *Nat. Commun.* **7**, 12389 (2016).
24. A. Tsaousi, H. Williams, C. A. Lyon, V. Taylor, A. Swain, J. L. Johnson, S. J. George, Wnt4/β-catenin signaling induces VSMC proliferation and is associated with intimal thickening. *Circ. Res.* **108**, 427–436 (2011).
25. X. Wang, Y. Xiao, Y. Mou, Y. Zhao, W. M. Blankesteijn, J. L. Hall, A role for the β-catenin/T-cell factor signaling cascade in vascular remodeling. *Circ. Res.* **90**, 340–347 (2002).
26. H. Williams, C. A. Mill, B. A. Monk, S. Hulin-Curtis, J. L. Johnson, S. J. George, Wn^{T2} and WISP-1/CCN4 induce intimal thickening via promotion of smooth muscle cell migration. *Arterioscler. Thromb. Vasc. Biol.* **36**, 1417–1424 (2016).
27. H. Williams, S. Slater, S. J. George, Suppression of neointima formation by targeting β-catenin/TCF pathway. *Biosci. Rep.* **36**, e00427 (2016).
28. G. K. Owens, M. S. Kumar, B. R. Wamhoff, Molecular regulation of vascular smooth muscle cell differentiation in development and disease. *Physiol. Rev.* **84**, 767–801 (2004).
29. K. Yamada, Y. Hori, S. Inoue, Y. Yamamoto, K. Iso, H. Kamiyama, A. Yamaguchi, T. Kimura, M. Uesugi, J. Ito, M. Matsuki, K. Nakamoto, H. Harada, N. Yoneda, A. Takemura, I. Kushida, N. Wakayama, K. Kubara, Y. Kato, T. Semba, A. Yokoi, M. Matsukura, T. Odagami, M. Iwata, A. Tsuruoka, T. Uenaka, J. Matsui, T. Matsushima, K. Nomoto, H. Kouji, T. Owa, Y. Funahashi, Y. Ozawa, E7386, a selective inhibitor of the interaction between β-catenin and CBP, exerts antitumor activity in tumor models with activated canonical Wnt signaling. *Cancer Res.* **81**, 1052–1062 (2021).
30. F. Yu, C. Yu, F. Li, Y. Zuo, Y. Wang, L. Yao, C. Wu, C. Wang, L. Ye, Wnt/β-catenin signaling in cancers and targeted therapies. *Signal Transduct. Target. Ther.* **6**, 307 (2021).
31. T. Valenta, M. Gay, S. Steiner, K. Draganova, M. Zemke, R. Hoffmans, P. Cinelli, M. Aguet, L. Sommer, K. Basler, Probing transcription-specific outputs of β-catenin in vivo. *Genes Dev.* **25**, 2631–2643 (2011).
32. O. Wendling, J. M. Bornert, P. Chambon, D. Metzger, Efficient temporally-controlled targeted mutagenesis in smooth muscle cells of the adult mouse. *Genesis* **47**, 14–18 (2009).
33. L. Madisen, T. A. Zwingman, S. M. Sunkin, S. W. Oh, H. A. Zariwala, H. Gu, L. L. Ng, R. D. Palmiter, M. J. Hawrylycz, A. R. Jones, E. S. Lein, H. Zeng, A robust and high-throughput Cre reporting and characterization system for the whole mouse brain. *Nat. Neurosci.* **13**, 133–140 (2010).
34. R. Kleszcz, A. Szymanska, V. Krajka-Kuzniak, W. Baer-Dubowska, J. Paluszczak, Inhibition of CBP/β-catenin and porcupine attenuates Wnt signaling and induces apoptosis in head and neck carcinoma cells. *Cell. Oncol. (Dordr.)* **42**, 505–520 (2019).
35. X. Sun, B. Mathew, S. Sammani, J. R. Jacobson, J. G. N. Garcia, Simvastatin-induced sphingosine 1-phosphate receptor 1 expression is KLF2-dependent in human lung endothelial cells. *Pulm. Circ.* **7**, 117–125 (2017).
36. B. Jung, H. Obinata, S. Galvani, K. Mendelson, B. S. Ding, A. Skoura, B. Kinzel, V. Brinkmann, S. Rafii, T. Evans, T. Hla, Flow-regulated endothelial S1P receptor-1 signaling sustains vascular development. *Dev. Cell* **23**, 600–610 (2012).
37. M. R. Bennett, S. Sinha, G. K. Owens, Vascular smooth muscle cells in atherosclerosis. *Circ. Res.* **118**, 692–702 (2016).
38. D. Nam, C. W. Ni, A. Rezvan, J. Suo, K. Budzyn, A. Llanos, D. Harrison, D. Giddens, H. Jo, Partial carotid ligation is a model of acutely induced disturbed flow, leading to rapid endothelial dysfunction and atherosclerosis. *Am. J. Physiol. Heart Circ. Physiol.* **297**, H1535–H1543 (2009).
39. Y. Wang, P. Lu, B. Wu, D. F. Riascos-Bernal, N. E. S. Sibinga, T. Valenta, K. Basler, B. Zhou, Myocardial β-catenin-BMP2 signaling promotes mesenchymal cell proliferation during endocardial cushion formation. *J. Mol. Cell. Cardiol.* **123**, 150–158 (2018).
40. D. Buechel, N. Sugiyama, N. Rubinstein, M. Saxena, R. K. R. Kalathur, F. Luond, V. Vafaizadeh, T. Valenta, G. Hausmann, C. Cantu, K. Basler, G. Christofori, Parsing β-catenin's cell adhesion and Wnt signaling functions in malignant mammary tumor progression. *Proc. Nat. Acad. Sci. U S A.* **118**, e2020227118 (2021).
41. A. Cantalupo, A. Gargiulo, E. Dautaj, C. Liu, Y. Zhang, T. Hla, A. Di Lorenzo, S1PR1 (sphingosine-1-phosphate receptor 1) signaling regulates blood flow and pressure. *Hypertension* **70**, 426–434 (2017).
42. A. Nitzsche, M. Poittevin, A. Benarab, P. Bonnin, G. Faraco, H. Uchida, J. Favre, L. Garcia-Bonilla, M. C. L. Garcia, P. L. Leger, P. Therond, T. Mathivet, G. Autret, V. Baudrie, L. Couty, M. Kono, A. Chevallier, H. Niazi, P. L. Tharaux, J. Chun, S. R. Schwab, A. Eichmann, B. Tavitian, R. L. Proia, C. Charriaut-Marlangue, T. Sanchez, N. Kubis, D. Henrion, C. Iadecola, T. Hla, E. Camerer, Endothelial S1P1 signaling counteracts infarct expansion in ischemic stroke. *Circ. Res.* **128**, 363–382 (2021).
43. K. Yanagida, C. H. Liu, G. Faraco, S. Galvani, H. K. Smith, N. Burg, J. Anrather, T. Sanchez, C. Iadecola, T. Hla, Size-selective opening of the blood–brain barrier by targeting endothelial sphingosine 1-phosphate receptor 1. *Proc. Nat. Acad. Sci. U S A.* **114**, 4531–4536 (2017).
44. K. A. Tran, X. Zhang, D. Predescu, X. Huang, R. F. Machado, J. R. Gothert, A. B. Malik, T. Valyi-Nagy, Y. Y. Zhao, Endothelial β-catenin signaling is required for maintaining adult blood–brain barrier integrity and central nervous system homeostasis. *Circulation* **133**, 177–186 (2016).
45. A. Cattelino, S. Liebner, R. Gallini, A. Zanetti, G. Balconi, A. Corsi, P. Bianco, H. Wolburg, R. Moore, B. Oreda, R. Kemler, E. Dejana, The conditional inactivation of the β-catenin gene in endothelial cells causes a defective vascular pattern and increased vascular fragility. *J. Cell Biol.* **162**, 1111–1122 (2003).
46. K. Hubner, P. Cabochette, R. Dieguez-Hurtado, C. Wiesner, Y. Wakayama, K. S. Grassme, M. Hubert, S. Guenther, H. G. Belting, M. Affolter, R. H. Adams, B. Vanhollebeke, W. Herzog, Wnt/β-catenin signaling regulates VE-cadherin-mediated anastomosis of brain capillaries by counteracting S1pr1 signaling. *Nat. Commun.* **9**, 4860 (2018).
47. K. P. Lee, S. Baek, S. H. Jung, L. Cui, D. Lee, D. Y. Lee, W. S. Choi, H. W. Chung, B. H. Lee, B. Kim, K. J. Won, DJ-1 is involved in epigenetic control of sphingosine-1-phosphate

receptor expression in vascular neointima formation. *Pflugers Arch.* **470**, 1103–1113 (2018).
48. C. M. Carlson, B. T. Endrizzi, J. Wu, X. Ding, M. A. Weinreich, E. R. Walsh, M. A. Wani, J. B. Lingrel, K. A. Hogquist, S. C. Jameson, Kruppel-like factor 2 regulates thymocyte and T-cell migration. *Nature* **442**, 299–302 (2006).
49. H. Lee, J. Deng, M. Kujawski, C. Yang, Y. Liu, A. Herrmann, M. Kortylewski, D. Horne, G. Somlo, S. Forman, R. Jove, H. Yu, STAT3-induced S1PR1 expression is crucial for persistent STAT3 activation in tumors. *Nat. Med.* **16**, 1421–1428 (2010).
50. V. R. Silva, T. O. Micheletti, G. D. Pimentel, C. K. Katashima, L. Lenhare, J. Morari, M. C. Mendes, D. S. Razolli, G. Z. Rocha, C. T. de Souza, D. Ryu, P. O. Prada, L. A. Velloso, J. B. Carvalheira, J. R. Pauli, D. E. Cintra, E. R. Ropelle, Hypothalamic S1P/S1PR1 axis controls energy homeostasis. *Nat. Commun.* **5**, 4859 (2014).
51. I. Josipovic, B. Pfluger, C. Fork, A. E. Vasconez, J. A. Oo, J. Hitzel, S. Seredinski, E. Gamen, D. M. Z. Heringdorf, W. Chen, M. Looso, S. S. Pullamsetti, R. P. Brandes, M. S. Leisegang, Long noncoding RNA LISPR1 is required for S1P signaling and endothelial cell function. *J. Mol. Cell. Cardiol.* **116**, 57–68 (2018).
52. C. Mosimann, G. Hausmann, K. Basler, β-Catenin hits chromatin: Regulation of Wnt target gene activation. *Nat. Rev. Mol. Cell Biol.* **10**, 276–286 (2009).
53. E. R. Reed, S. A. Jankowski, A. J. Spinella, V. Noonan, R. Haddad, K. Nomoto, J. Matsui, M. V. Bais, X. Varelas, M. A. Kukuruzinska, S. Monti, β-Catenin/CBP activation of mTORC1 signaling promotes partial epithelial-mesenchymal states in head and neck cancer. *Transl. Res.* **260**, 46–60 (2023).
54. Y. Kanda, H. Ohata, T. Miyazaki, H. Sakai, Y. Mori, D. Shiokawa, A. Yokoi, T. Owa, A. Ochiai, K. Okamoto, NF-κB suppression synergizes with E7386, an inhibitor of CBP/β-catenin interaction, to block proliferation of patient-derived colon cancer spheroids. *Biochem. Biophys. Res. Commun.* **586**, 93–99 (2022).
55. Y. Higuchi, C. Nguyen, N. O. Chimge, C. Ouyang, J. L. Teo, M. Kahn, E7386 is not a specific CBP/β-catenin antagonist. *Curr. Mol. Pharmacol.* **17**, e290523217409 (2023).
56. H. Sabbineni, A. Verma, S. Artham, D. Anderson, O. Amaka, F. Liu, S. P. Narayanan, P. R. Somanath, Pharmacological inhibition of β-catenin prevents EndMT in vitro and vascular remodeling in vivo resulting from endothelial Akt1 suppression. *Biochem. Pharmacol.* **164**, 205–215 (2019).
57. M. Rong, S. Chen, R. Zambrano, M. R. Duncan, G. Grotendorst, S. Wu, Inhibition of β-catenin signaling protects against CTGF-induced alveolar and vascular pathology in neonatal mouse lung. *Pediatr. Res.* **80**, 136–144 (2016).
58. D. Alapati, M. Rong, S. Chen, D. Hehre, S. C. Hummler, S. Wu, Inhibition of β-catenin signaling improves alveolarization and reduces pulmonary hypertension in experimental bronchopulmonary dysplasia. *Am. J. Respir. Cell Mol. Biol.* **51**, 104–113 (2014).
59. V. Brault, R. Moore, S. Kutsch, M. Ishibashi, D. H. Rowitch, A. P. McMahon, L. Sommer, O. Boussadia, R. Kemler, Inactivation of the β-catenin gene by Wnt1-Cre-mediated deletion results in dramatic brain malformation and failure of craniofacial development. *Development* **128**, 1253–1264 (2001).
60. T. A. Seimon, Y. Wang, S. Han, T. Senokuchi, D. M. Schrijvers, G. Kuriakose, A. R. Tall, I. A. Tabas, Macrophage deficiency of p38α MAPK promotes apoptosis and plaque necrosis in advanced atherosclerotic lesions in mice. *J. Clin. Invest.* **119**, 886–898 (2009).
61. O. O. Onyema, Y. Guo, B. Mahgoub, Q. Wang, A. Manafi, Z. Mei, A. Banerjee, D. Li, M. H. Stoler, M. T. Zaidi, A. G. Schrum, D. Kreisel, A. E. Gelman, E. A. Jacobsen, A. S. Krupnick, Eosinophils downregulate lung alloimmunity by decreasing TCR signal transduction. *JCI Insight* **4**, e128241 (2019).

Acknowledgments: We thank J. G.N. Garcia at University of Arizona for providing the pGL3-*S1PR1*-promoter plasmid. **Funding:** This work was supported by American Heart Association Postdoctoral Fellowship 874619 (to G.H.O.-P.), American Heart Association Career Development Award 19CDA34660217, and NIH grants R01HL163192 (to D.F.R.-B.), R35HL135821 (to T.H.), and R01HL128066 (to N.E.S.S.). **Author contributions:** All authors contributed to and have approved the manuscript. Conceptualization: N.E.S.S., D.F.R.-B., and G.H.O.-P. Methodology: G.H.O.-P., S.L., A.M., G.R., G.C.F., A.Q., S.J., V.A., D.P., T.V., K.B., and T.H. Supervision: N.E.S.S. and D.F.R.-B. Writing—original draft: G.H.O.-P. Writing—review and editing: G.H.O.-P., D.F.R.-B., and N.E.S.S. **Competing interests:** The authors declare that they have no competing interests. **Data and materials availability:** RNA-seq data for this study have been deposited in the database Dryad and can be found at https://datadryad.org/stash/share/AOhXJz7874MfiYgnSDnTFPOLU8RHyN1HzVbUrFA2vhI. All data needed to evaluate the conclusions in the paper are present in the paper and/or the Supplementary Materials. Inquiries regarding mouse line availability should be directed as follows: (i) *Acta2-CreER*^{T2} line, P. Chambon (chambon@igbmc.fr) and (ii) *Ctnnb1*$^{\Delta C/flox}$ line, K.B. (konrad.basler@mls.uzh.ch).

Submitted 3 February 2023
Accepted 7 February 2024
Published 13 March 2024
10.1126/sciadv.adg9278